CALIFORNIA STATE UNIVERSITY, NORTHRIDGE

PROTEIN FOLDING: PLANAR CONFIGURATION SPACES OF DISC ARRANGEMENTS AND HINGED POLYGONS

A thesis submitted in partial fulfillment of the requirements for the degree of
Master of Science in Applied Mathematics

by

Clinton Bowen

August 2014

The thesis of Clinton Bowen is approved:

Dr. Silvia Fernandez	Date
Dr. John Dye	Date
Dr. Csaba Tóth, Chair	Date

California State University, Northridge

ABSTRACT

PROTEIN FOLDING: PLANAR CONFIGURATION SPACES OF DISC ARRANGEMENTS AND HINGED POLYGONS

By

Clinton Bowen

Master of Science in Applied Mathematics

Chapter 1

Background

We consider four decision problems surrounding graph theory and geometry. The graph theory based problems involve polygonal linkages and the geometry based problems involve something called a contact graph of disks. In each problem, we decide whether a polygonal linkage or contact graph has a certain realization in the plane.

This thesis first presents preliminary information needed to pose our four problems, then we formally pose each problem and then provide the hardness results in all four cases. We show that all four problems are intractable, or NP hard (see definition below).

1.1 Graphs

A *graph* is an ordered pair $G = (V, E)$ comprising of a set of vertices V and a set of edges E. An edge is a two element subset of V. Note that with this definition of an edge it is not possible to have one element subset of V as an edge (sometimes referred to as a self-adjacent edge or loop). The *degree* of a vertex v is the number of edges that v is an element of. Vertices are said to be *adjacent* if they form an edge in E. *Neighbors* of a vertex v are the vertices adjecent to v. Edges are said to be adjacent if they share a vertex.

A *simple graph* has no self-adjacent vertices. In this thesis every graph is a simple graph. Given a graph $G = (V, E)$, a set of vertices $S \subset V$ is *independent* if no two vertices in S are joined by an edge. A *vertex cover* of a graph $G = (V, E)$ is a set of vertices $S \subset V$ if every edge $e \in E$, has at least one end corresponding in S. If $G' = (V', E')$ is a graph such that $V' \subset V$ and $E' \subset E$, then G' is a *subgraph* of G.

To formally show when two graphs are the same, we use the concept of graph isomorphism. Two graphs $G_1 = (V_1, E_1)$ and $G_2 = (V_2, E_2)$ are *isomorphic* if there exists a bijective function $f : V_1 \mapsto V_2$ such that for any two vertices $u, v \in V_1$, we have $\{u, v\} \in E_1$ if and only if $(f(u), f(v)) \in E_2$. See an example in Table **??** and Figure 1.21.

Graph	Vertices	Edges
G_1	$\{a,b,c,d,e\}$	$\{(a,b),(b,c),(c,d),(d,e),(e,a)\}$
G_2	$\{1,2,3,4,5\}$	$\{(1,2),(2,3),(3,4),(4,5),(5,1)\}$

Table 1.1: Two graphs that are isomorphic with the alphabetical isomorphism $f(a) = 1$, $f(b) = 2$, $f(c) = 3$, $f(d) = 4$, $f(e) = 5$.

Figure 1.1: This figure depicts the graph isomorphism shown in Table **??** between V_1 and V_2.

To visualize a graph, G, we create a drawing Γ, of G. The *drawing* of a graph $G = (V, E)$ is an injective mapping $\Pi : V \mapsto \mathbb{R}^2$ which maps vertices to distinct points in the plane and for each edge $\{u, v\} \in E$, a continuous, injective mapping $c_{u,v} : [0,1] \mapsto \mathbb{R}^2$ such that $c_{u,v}(0) = \Pi(u)$, $c_{u,v}(1) = \Pi(v)$, and the curve $c_{u,v}$ does not pass through any other vertex in V. In this thesis, we will strictly work with straight line drawings where all $c_{u,v}$ are straight line segments unless specified otherwise. Kuratowski's theorem characterizes finite

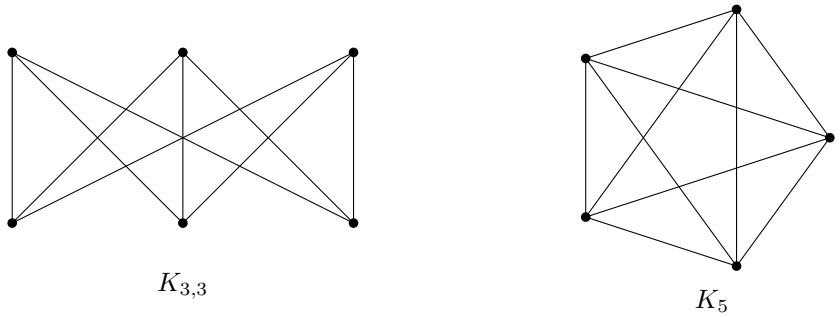

Figure 1.2: The K_5 and $K_{3,3}$ drawn in the plane.

planar graphs. A finite graph is planar if and only if it does not contain a subgraph that is a subdivision of K_5 or $K_{3,3}$ [15]. Figure 1.2 shows a drawing of K_5 and $K_{3,3}$. Two edges in a drawing *cross* if they have a common interior point. The *crossing number* of a graph is the smallest number of edge crossings for a graph over all drawings. A drawing is said to be *planar* if no two distinct edges cross [3]. A planar drawing is also called an *embedding*. Two embeddings of a graph G are *equivalent* if for every vertex the counter-clockwise order of neighbors are the same.A combinatorial *embedding* is a planar drawing with a corresponding counter-clockwise order of the neighbors of each vertex. An orientation preserving rigid transformation (i.e., rotation

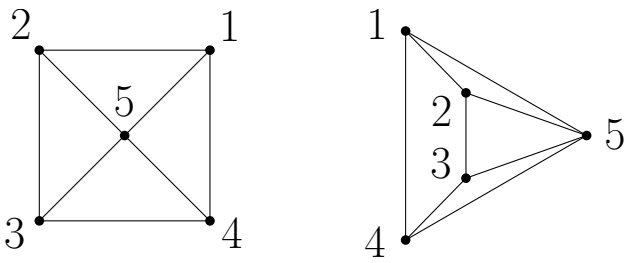

Figure 1.3: Here is a wheel graph, W_5, in two separate drawings with the same counterclockwise ordering of neighbors for each vertex.

and translation) map an embedding to an equivalent embedding. Reflections reverse the counter-clockwise order around each vertex.

Figure 1.3 depicts two different drawings of the wheel graph W_5.The drawings have the followings counterclockwise order of neighbors for each vertex: Referencing table **??** and Figure 1.3, we realize that the two drawings of W_5 are equivalent.

Vertex	Left & Middle Drawing	Right Drawing
1	$(2,5,4)$	$(4,5,2)$
2	$(3,5,1)$	$(1,5,3)$
3	$(2,4,5)$	$(5,4,2)$
4	$(1,5,3)$	$(3,5,1)$
5	$(2,3,4,1)$	$(4,3,2,1)$

Table 1.2: A table showing the counter-clockwise circular ordering of neighbors for the left and right drawing in Figure 1.3. Note that the permutation cycles are equivalent for the right and left drawings.

1.1.1 Trees

A *path* is a sequence of vertices in which every two consecutive vertices are connected by an edge.

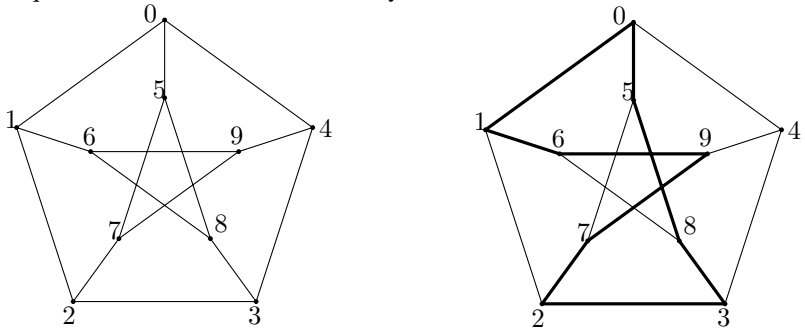

Figure 1.4: An embedding of the Peterson graph with a simple cycle of (2,7,9,6,1,0,5,8,3).

A *simple cycle* of a graph is a sequence, $(v_1, v_2, \ldots, v_{t-1}, v_t)$, of distinct vertices such that every two consecutive vertices are connected by an edge, and the last vertex, v_t, connects to v_1 (see Figure 1.4). A graph is *connected* if for any two vertices, there exists a path between the two points. A *tree* is a graph that has no simple cycles and is connected (see Figure 1.5). Every tree is planar. A *forest* is a disjoint union of trees.

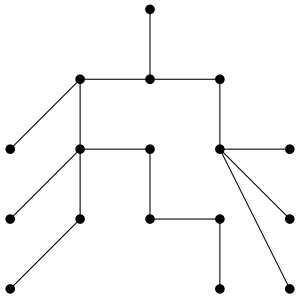

Figure 1.5: An example of a tree.

An *ordered tree* is a tree T together with a cyclic order of the neighbors for each vertex (see Figure 1.6).

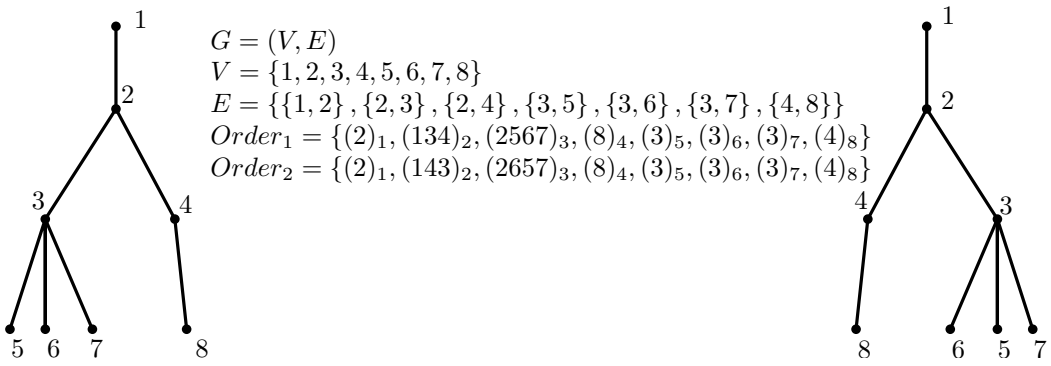

Figure 1.6: A tree with two embeddings with different cyclic orderings around vertices.

Embeddings of ordered trees are combinatorially equivalent if for each node the counter-clockwise ordering of adjacent nodes are the same.

1.2 Linkages

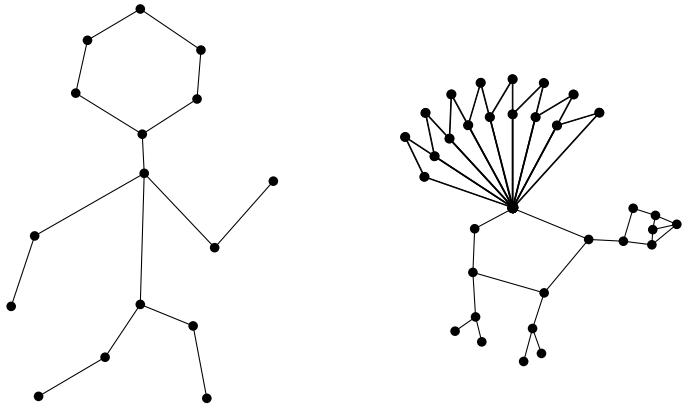

Figure 1.7: Here are skeleton drawings of a human and a turkey. When animating skeletons, one tends to make sure that the lengths of the skeleton segments are kept the same length throught the animation. Otherwise, the animation may depart from what is ideally understood of skeletal motions.

When graph drawings model physical objects, other qualities about the graph can be contextualized in a geometric sense. Distance, angular relationships and other geometric qualities may be relevant. In any drawing, edges have length, angles formed by adjacent edges, and so on. In this thesis we are interested in the inverse problem where we would like to embed a graph with specific geometric properties, for example, an embedding with specified edge lengths. This motivates the following definition. A *length assignment* of a graph $G = (V, E)$ is a function $\ell : E \mapsto \mathbb{R}^+$. If $\ell(e)$ is the length of an edge e, $\ell(e)$ must be strictly positive in a drawing, otherwise it may result in two distinct vertices with the same coordinates. Similar to combinatorial embeddings which is an equivalence class of embeddings of the same counter-clockwise order of vertices, we can also define an equivalence class of drawings with the same length assignment. A *linkage* is a graph $G = (V, E)$ with a length assignment $\ell : E \mapsto \mathbb{R}^+$ (e.g., see Figure **??**).

1.3 Polygonal Linkages

A generalization of linkages is a polygonal linkage where edges of given lengths are replaced with rigid polygons. Formally, a *polygonal linkage* is an ordered pair $(\mathscr{P}, \mathscr{H})$ where $\mathscr{P}$ is a finite set of polygons and $\mathscr{H}$ is a finite set of hinges; a *hinge* $h \in \mathscr{H}$ corresponds to two or more points on the boundary of distinct polygons in $\mathscr{P}$. A *realization of a polygonal linkage* is an interior-disjoint placement of congruent copies of the polygons in $\mathscr{P}$ such that the copies of a hinge are mapped to the same point (e.g., Figure

1.8). A *realization of a polygonal linkage with fixed orientation* is a realization in which each polygon is

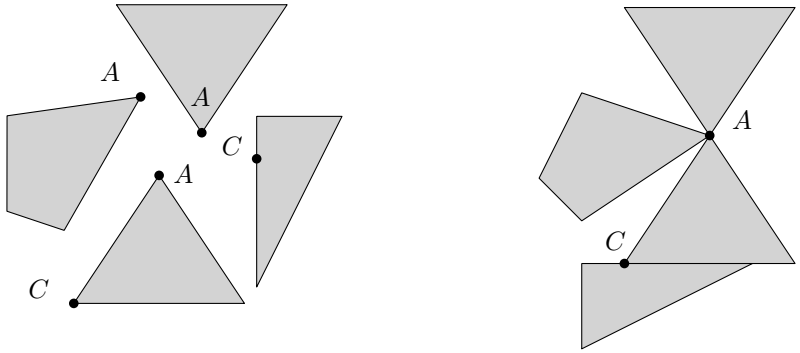

Figure 1.8: (a) A polygonal linkage with a non-convex polygon and two hinge points corresponding to three polygons. Note that hinge points correspond to two distinct polygons.(b) Illustrating that two hinge points can correspond to the same boundary point of a polygon.

translated and rotated copy of a polygon in $\mathscr{P}$; at each hinge the incident polygons are in a given counter-clockwise order (refer to Figure **??**). Note that oriented polygonal linkage realizations do not allow for

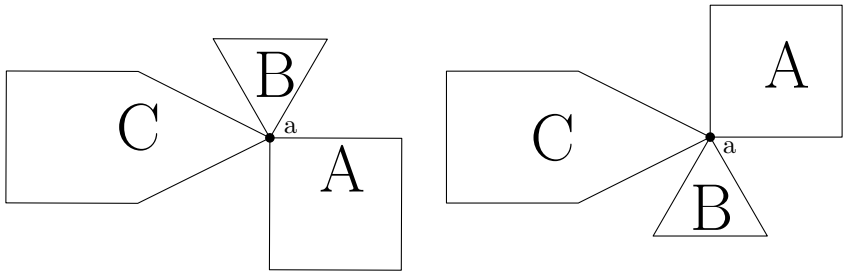

Figure 1.9: Two realizations of the same polygonal linkage with that differ in the counter-clockwise order of polygons around vertex *a*.

reflection transformations of polygons in $\mathscr{P}$.

These two realization types allow one to pose two different problems, the realizability problem for polygonal linkages and the realizability problem for polygonal linkages with fixed orientation:

Problem 1 (Realizibility Problem for Polygonal Linkages). Given a polygonal linkage, does it have a realization?

Problem 2 (Realizibility Problem for Polygonal Linkages with Fixed Orientation). Given a polygonal linkage with fixed orientation, does it have a realization?

Not every polygonal linkage has a realization. Consider the 7 congruent copies of an equilateral triange with a common hinge point in Figure 1.10. To show it does not have a realization, suppose it is realizable. Each angle of every triangle is $\frac{\pi}{3}$ radians. The sum of 7 angles formed by the triangles is $\frac{7\pi}{3} > 2\pi$. The total radian measure around A is 2π. The contradiction is that the sum of 7 angles formed by the triangles in an interior disjoint placement is $\frac{7\pi}{3}$. The polygonal linkage of Figure 1.10 would overlap itself and does not have a realization.

There are polygonal linkages that admit realizations but every realization requires rotation. Figure **??** show the congruent copies of the polygons A, B, C, and D in two different configurations, the far right is a realization, the middle fails to be a realization because of the interiors of B and D intersecting and the left

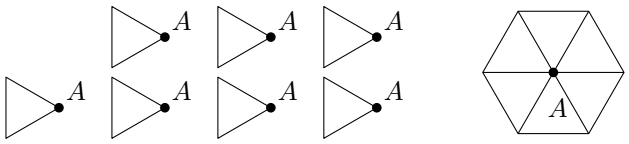

Figure 1.10: Here we have 7 congruent copies of an equilateral triangle with a hinge point of A. The polygonal linkage is not realizable. The best we can realize is at most 6 congruent copies of an equilateral triangle with the hinge point of A in the plane.

showing the polygons in $\mathscr{P}$. In fact, this polygonal linkage cannot admit a realization with fixed orientation. Indeed this polygonal linkage cannot satisfy Problem 2, suppose there is a realization with fixed orientation. Without loss of generality, fix the placement of C. A, B, and D have unique placement around triangle C. In this placement C and D overlap. Figure **??**, satisfies Problem 1 but not Problem 2. The far right is a realization

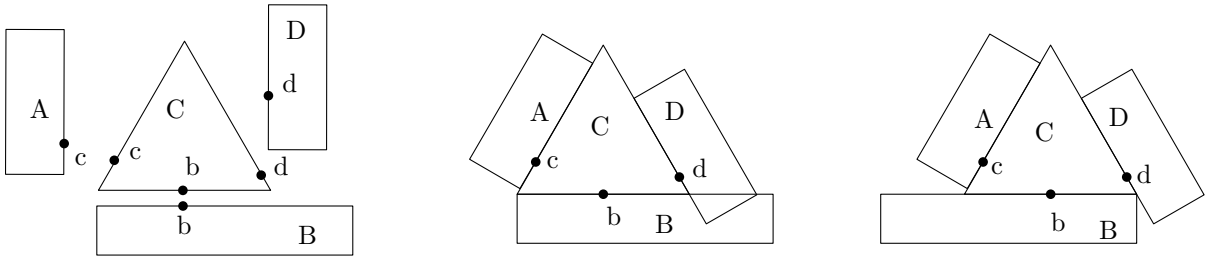

Figure 1.11: This example shows yet another example where two realizations of the same polygonal linkage. One realization where there is an intersection and another where there isn't an intersection.

but with polygon B reflected.

Figure **??** does not quite get at the heart of the challenge with Problem 1 because the counter-clockwise order of the polygons around hinges is not considered.

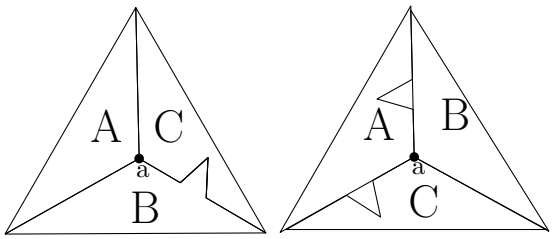

Figure 1.12: Here we have two realizations of a polygonal linkage with two different counter-clockwise order (C,B,A) and (B,C,A) respectively. Note that the placement with ordering (B,C,A) has an overlap.

Figure **??** shows three polygons with a common hinge. In the counter-clockwise order (A,B,C), the polygonal linkage admits a realization whereas in the counter-clockwise order (A,C,B), it does not admit a realization. The examples above show that answers to Problem 1 and 2 could be yes or no; the answer could be negative for various reasons. Sections 2 and 3 of this thesis address the computational complexity of solving Problems 1 and 2. We show that both problems are intractable.

1.3.1 Geometric Dissections

Hilbert's third problem asks: given any two polyhedra of equal volume, is it always possible to cut the first into finitely many polyhedral pieces which can be reassembled to yield the second [2]? In three dimensions the answer is no however for two dimensions it is true [22].

The Wallace-Bolyai-Gerwien Theorem simply states that two polygons are congruent by dissection iff they have the same area. A *dissection* being a collection of smaller polygons whose interior disjoint union forms a polygon. Hinged dissections of a polygon P is a polygonal linkage that admits a realization that forms P. Demaine et. al. [1] showed that any two polygons of the same area have a common hinged dissection where polygonal pieces must hinge together at vertices to form a connected realization and that there exists a continuous motion between the two realizations (refer to section 1.5.3). The was an outstanding problem for many years until 2007.

The Haberdasher Puzzle was proposed in 1902 by Henry Dudeney: can a square and an equilateral triangle of the same area have a common dissection into four pieces?

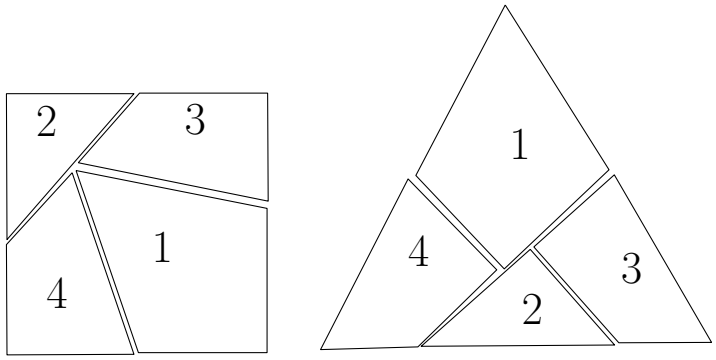

Figure 1.13: The Haberdasher Puzzle was proposed in 1902 and solved in 1903 by Henry Dudeny. The dissection is for polygons that forms a square and equilateral traingle

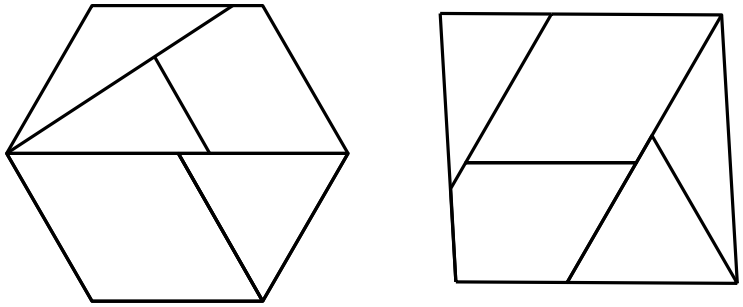

Figure 1.14: Two configurations of polygonal linkage where the polygons touch on boundary segments instead of hinges. These two realizations of the polygonal linkage are invalid to our definitions.

Geometric dissections are closely related to polygonal linkages. Figure 1.14 shows two arrangements of the same polygons to form a hexagon and a square. The polygons are not hinged and are arranged in differing order. The polygons are merely tiled together to form the hexagon and square. Figure 1.15, shows the Haberdasher problem with hinges. This makes the Haberdasher problem as a type of polygonal linkage where the polygons are free to move about their hinge points and take the form of a triangle or square.

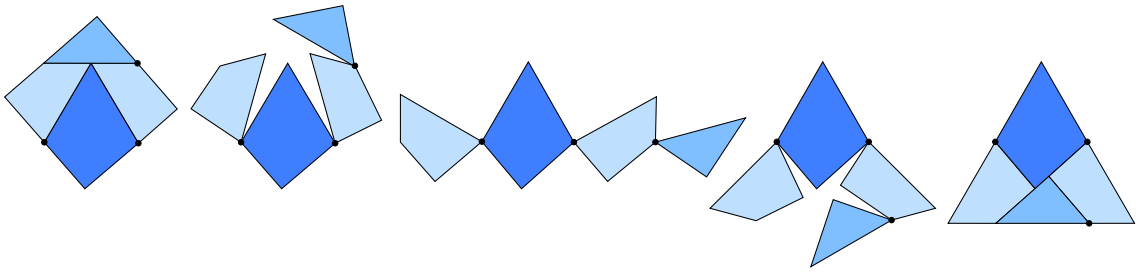

Figure 1.15: This shows the Haberdasher problem in the form of polygonal linkage [1]. This is a classic example of two polygons of equal area that have a common hinged dissection.

1.4 Disk Arrangements

A *disk arrangement* is a set of interior disjoint disks, D. If for any pair of disks in D intersect at a boundary point, they are said to be in contact (kissing). A *contact graph* $G = (V, E)$ corresponding to a given

Figure 1.16: This example represents a disk arrangement and its contact graph.

disk arrangement where there is a bijection $b_V : V \mapsto D$ and a bijection that maps an edge $e_{i,j} \in E$ to an interior disjoint pair of disks $d_i, d_j \in D$ (see Figure 1.16). Given a disk arrangement, the contact graph can be thought of as a linkage because the distance between two kissing disk equal the sum of radii. However if the two disks don't kiss, the distance between their centers is strictly greater than the sum of their radii. Given a

disk arrangement, the contact graph can be thought of as a linkage because the distance between two kissing disk equal the sum of radii. However if the two disks don't kiss, the distance between their centers is strictly greater than the sum of their radii.

Koebe's theorem states that for every planar graph G, there exists a planar disk arrangement whose contact graph is G [14]. This motivates the question of whether a planar graph G is a contact graph of a disk arrangement with given radii. The radii can be given by a weight function. Let $\omega : V \mapsto \mathbb{R}^+$ be the *weight function*. ω assigns a weight to each vertex in V. Let $\Pi : V \mapsto \mathbb{R}^2$ be that planar mapping of vertices.

For planar graphs with positive weighted vertices, we pose two realizability problems:

Problem 3 (Unordered Realizibility Problem for a Contact Graph). Given a planar graph with positive weighted vertices, is it a contact graph of some disk arrangement where the radii equal the vertex weights?

Problem 4 (Ordered Realizibility Problem for a Contact Graph). Given a planar graph with positive weighted vertices and a combinatorial embedding, is it a contact graph of some disk arrangement where the radii equal the vertex weights and the counter-clockwise order of neighbors of each disk is specified by the combinatorial embedding?

An instance of Problem 3 is shown in Figure 1.16 where the cycle graph C_5 is the contact graph of unit disks. It is not difficult to see that there exists a planar graph with positive weights with no realizable disk arrangement. Consider the a star graph with 6 leafs, each vertex with unit weight. In any realization, the angle between two consecutive edges must be greater than $\frac{\pi}{3}$. The sum of 6 angles is 2π however, the sum of 6 consecutive angles is greater than 2π. The contradiction shows that no realization is possible (refer to Figure **??**). Note that with the wheel graph W_7 is realizable as a contact graph of unit disks.

Every path with arbitrary positive radii is realizable as a contact graph, place the vertices on a line. We show that not all binary trees are realizable, even with unit disks.Consider the balanced binary trees of depth i $\{T_i\}_{i=1}^{\infty}$ with unit weights on the vertices (see Figure 1.18). These trees are not realizable for sufficiently large i. Let i be a positive integer and suppose that T_i is a contact graph of unit disks. The balanced binary

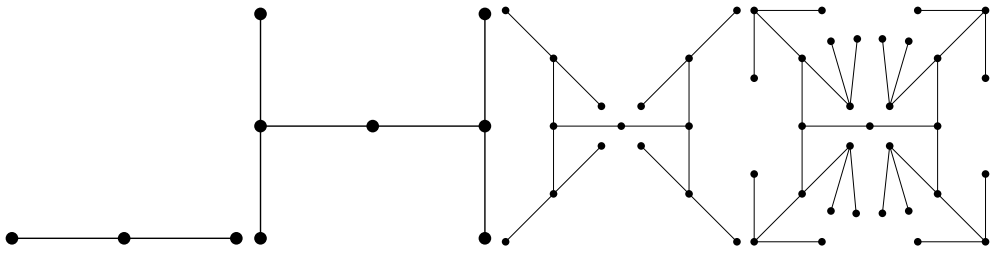

(a) Binary tree T_2. (b) Binary tree T_3. (c) Binary tree T_4. (d) Binary tree T_5.

Figure 1.17: We show the linkages T_2 through T_5 with distance 2 between adjacent vertices.

tree T_i has $2^i - 1$ vertices. The total area of the disks is $\left(2^i - 1\right)^2 \cdot \pi$. We now derive an upper bound for this area. Suppose the disk corresponding to the root of the tree is centered at the origin. The centers of the disks at level j are at a distance at most $2 \cdot (j-1)$ away from the origin. The centers of all disks are at distance at most $2 \cdot (i-1)$ away from the origin. All unit disks are contained in a disk of radius $2i-1$ centered at the origin. The total area of the disks is at most $(2i-1)^2$. A upper bound of the total area of the disk arrangement is the area of the bounding box of the disks. The upper bound of the

Figure **??** shows the first four non-trivial trees as a contact graph of unit disks. Every disk at level up to i is contained in a disk of radius $2 \cdot i - 1$ centered at the origin. The total area of the disk arrangement is $(2 \cdot i - 1)^2 \cdot \pi$. When $i \geq 8$ we have a contradiciton.

There are instances where a planar graph with weights admits a realization but the cyclic order of neighbors may not be the same as the combinatorial embedding. Define G as follows: start with a star centered

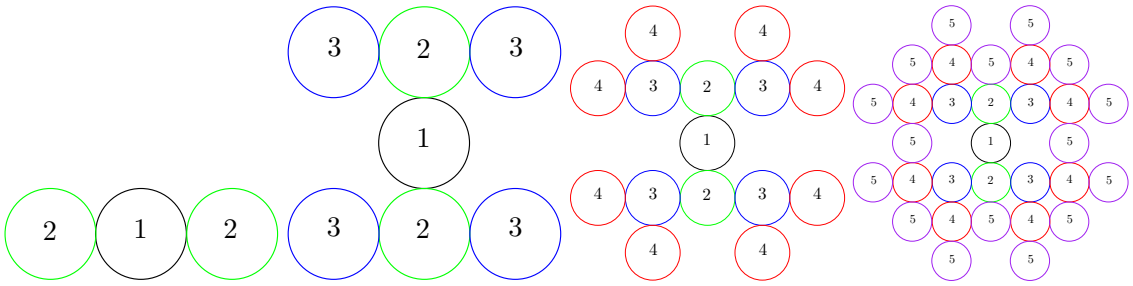

(a) A disk arrangement with two layers of disks (b) A disk arrangement with three layers of disks (c) A disk arrangement with four layers of disks (d) A disk arrangement with five layers of disks

Figure 1.18: For $i = 2,3,4,5$ the tree T_i is a contact graph of unit disks.

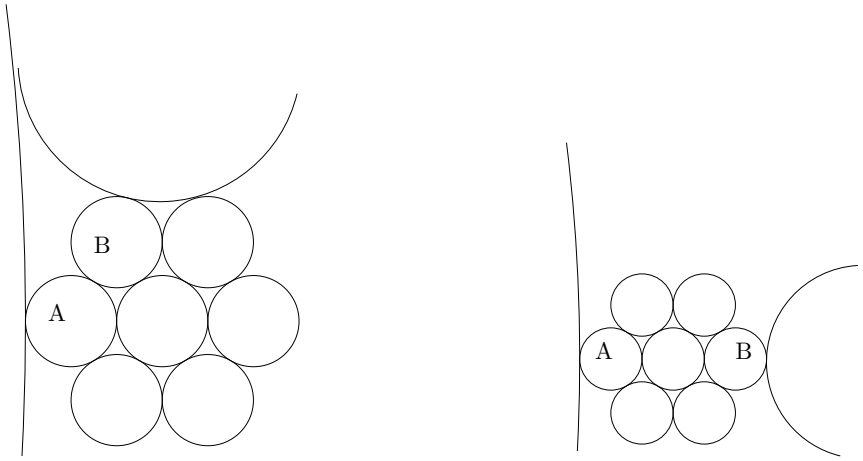

Figure 1.19: Consider these two ordered disk arrangements where A and B are in the concentric rings of disks. The large disks are in contact to A and B respectively. If A and B are adjacent, then there is a restriction of how large the size of the disks can be that are attached to them as seen in on the left. Whereas if A and B are not adjacent in this disk arrangment as shown on the right, the size of the kissings disks could be arbitrarily large.

at C and with 6 leafs, A_1 through A_6; attach two leafs, B_1 and B_2, to A_1 and A_2 respectively (see Figure **??**). Let the weight of C be $1+\varepsilon$ for sufficiently small $\varepsilon > 0$. The neighbors of C have unit weight. The weights of the two leaves have weight $\frac{1}{\varepsilon}$/ The right of Figure **??**) shows a realization where A_1 and A_2 are in opposite position of the counter-clockwise order around C. If A_1 and A_2 are required to be consecutive in the counter-clockwise order around C, there is no realization.

Suppose there is a realization where $A_1,\ldots,A_6$ are in the counter-clockwise order around C (see Figure **??**). If $\varepsilon > 0$ is sufficiently small, then the centers of of $A_1,\ldots,A_6$ are arbitrarily close to the vertices of a regular hexagon. Consider the common tangent lines between A_1 and B_1 and A_2 and B_2. The possible position of tangent line between A_1 and B_1 ranges from the common tangent line of A_1 and A_6 to the common tangent line of A_1 and A_2. Similarly, The possible position of tangent line between A_2 and B_2 ranges from the common tangent line of A_2 and A_3 to the common tangent line of A_1 and A_2. In any position, the common tangent lines between A_1 and B_1 and A_2 and B_2 intersect. If $\frac{1}{\varepsilon}$ is sufficiently large, then the disks D_1 and D_2 also intersect. This contradicts that there is a realization. Figure **??** shows how an ordered contact graph may

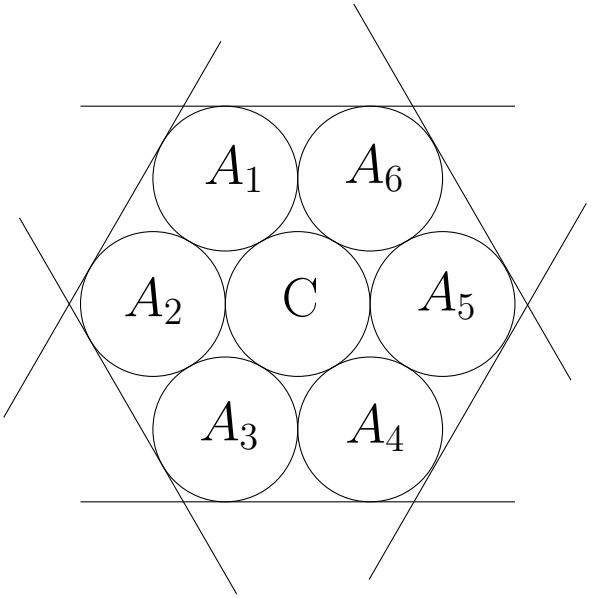

Figure 1.20: This example represents a disk arrangement and its contact graph.

not be realizable. On the left, it shows a limitation on the weights of the disks that are in contact with disks A and B. On the right, the figure shows the order where A and B are on opposing ends of the ring of disks and can allow of arbitrary size of wieghted disks in contact with A and B.

1.5 Configuration Spaces

Just as one can compose colors or forms, so one can compose motions.

Alexander Calder, 1933

Recall Figure 1.15 illustrating the hinged dissection that formed a square and triangle and several drawings of the hinged dissections that simulate the motion of moving the polygons around the hinge points to form each shape. The set of all drawings in that motion represents the *configuration space* for that polygonal linkage. In this section we will formally describe the configuration space for each object we've drawn thus far.

1.5.1 Configuration Spaces of Graph Drawings

Recall that for a graph drawing we have an injective mapping $\Pi : V \mapsto \mathbb{R}^2$ which maps vertices to distinct points in the plane and for each edge $\{u,v\} \in E$, a straight line segment, $c_{u,v} : [0,1] \mapsto \mathbb{R}^2$ such that $c_{u,v}(0) = \Pi(u)$ and $c_{u,v}(1) = \Pi(v)$, and does not pass through other vertices. For each vertex of G, the embedding of the vertex lies in the plane, i.e. $\Pi(v) \in \mathbb{R}^2$. By enumerating each vertex of G, e.g. $v_1, v_2, \ldots, v_k, \ldots, v_n$, we can create a projection mapping from $\mu : \Pi \mapsto \mathbb{R}^{2|V|}$ where the corresponding coordinates of $\Pi(v_k)$ are in the $(2k)^{\text{th}}$ and $(2k+1)^{th}$ coordinates in $\mathbb{R}^{2|V|}$. $\mu(\Pi)$ is a configuration. The configuration space is the set of $\mu(\Pi)$ for all drawings Π.

1.5.2 Configuration Spaces of Linkages

Consider drawings of a graph that respects the length assignment. A *realization* of a linkage, (G,ℓ), is a drawing of a graph, Π, such that for every edge $\{u,v\} \in E$, $\ell(\{u,v\}) = |\Pi(u) - \Pi(v)| = |\Pi(v) - \Pi(u)|$. A *plane realization* is a plane drawing with the property, $\ell(\{u,v\}) = |\Pi(u) - \Pi(v)|$. First let's define the space of realizations for a corresponding linkage, i.e.:

$$P_{(G,\ell)} = \left\{ \Pi_{(G,\ell)} \,|\forall \{u,v\} \in E,\, \ell(\{u,v\}) = |\Pi(u) - \Pi(v)| \right\}$$

With respect to P, we can establish a *configuration space* that allows one to study problems of motion. For each vertex of G, the drawing of the vertex lies in the plane, i.e. $\Pi(v) \in \mathbb{R}^2$. By enumerating each vertex of G, e.g. $v_1, v_2, \ldots, v_k, \ldots, v_n$, we can create a projection mapping from $\mu : P \mapsto \mathbb{R}^{2|V|}$ where the corresponding coordinates of $\Pi(v_k)$ are in the $(2k)^{\text{th}}$ and $(2k+1)^{th}$ coordinates in $\mathbb{R}^{2|V|}$. The configuration space is $\mu(P)$.

Using standard definitions from real analysis, we can begin to pose problems about linkages with respect to a corresponding configuration space. We define a path $\gamma : [0,1] \mapsto \mu(P)$ where $\gamma(0)$ corresponds the the projection of a realization of a linkage Π_0 and $\gamma(1)$ corresponds to another realization of a linkage Π_1. If for any two elements $a, b \in \mu(P)$ that there exists a continuous path γ such that $\gamma(0) = a$ and $\gamma(1) = b$, $\mu(P)$ is said to be path connected. For γ to be continuous we would have that for every $\varepsilon > 0$, there exists a $\delta > 0$ such that if $x, y \in [0,1]$ and $|x - y| < \delta$ then $||\gamma(x) - \gamma(y)|| < \varepsilon$. γ can be thought of as an animation of drawings that starts at $\gamma(0)$ and ends at $\gamma(1)$. To ask if $\mu(P)$ is a connected space, is to ask if $\mu(P)$ is connected in $\mathbb{R}^{2|V|}$. The Carpenter's Rule states that every realization of a path linkage can be continuously moved (without self-intersection) to any other realization [8, 21]. In other words, the realization space of such a linkage is always connected.

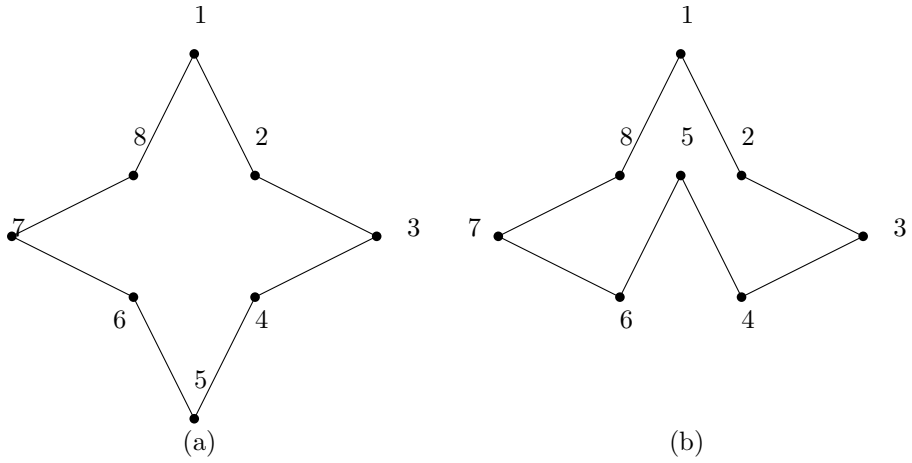

Figure 1.21: (a) and (b) show a linkage in two embeddings. Any realization of a path can be continuously moved without self-intersection to any other realizations.

1.5.3 Configuration Spaces of Polygonal Linkages

Recall a realization of a polygonal linkage is an interior-disjoint placement of congruent copies of the polygons in $\mathscr{P}$ such that the copies of a hinge are mapped to the same point (e.g., Figure 1.8). First consider the set of all realizations for the polygonal linkage. $(\mathscr{P}, \mathscr{H})$ and call it P. For any realization $R \in P$, the parameterization $\mu : R \mapsto \mathbb{R}^{2m}$ where m is the number of distinct vertices in $\mathscr{P}$. The configuration space is the set $\mu(P)$.

1.5.4 Configuration Spaces of Disk Arrangements

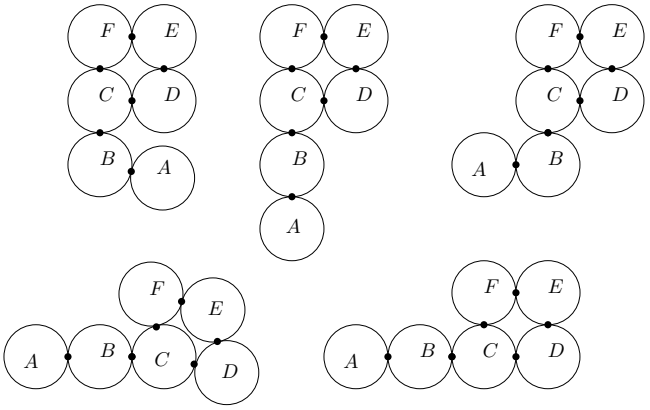

Figure 1.22: An example of a disk arrangement where A and B have a large range of freedom to move around. C, D, E, and F are limited in their range of motion to due to their hinge points.

Consider the set of realizations P for a given disk arrangement $\mathscr{D} = \{D_i\}_{i=1}^{n}$. For any realization $R \in P$, there exists a corresponding contact graph, C. The configuration spaces of $\mathscr{D}$ are sets of $R \in P$ that are classified by the equivalent contact graphs, i.e. if R_1, $R_2 \in P$ and their corresponding contact graphs C_1 and C_2 have a graph isomorphism, ϕ, then R_1 and R_2 belong to the same configuration space.

x

1.6 Algorithm Complexity

Algorithms are a list of instructions executed with a given input. The efficiency of an algorithm can be measured in terms of the amount of resources it uses such as time, memory, and power. Ideally, a desirable algorithm would primarily have a small run time and secondarily utilize a small amount of resources.

The time and space used by an algorithm is measured with units defined by a model of computation. The actual running time of an algorithm depend on a variety of factors for example: the processor, the hardware, the temperature, etc. Mathematical models of computation have been developed to measure running time of algorithms independent of the machine it runs on. One of the oldest and most popular models is the random access machine (RAM) model. RAM measures the unit of space in the number of words used where each word can store an arbitrary integer. In the real RAM, each word can store an arbitrary real number. The units of time is measured in the number of arithmetic operations and number of memory accesses (read or write).

The *running time* of an algorithm on a given input, is the time it takes to terminate.The *worst-case* running time is the largest running time over all inputs of a given size N. It is a function of N, it is usually monotonically increasing function since larger inputs tend to take more time to process. The key parameter of the efficiency of an algorithm is the growth rate of its worst case running time in terms of N. An algorithm is said to be *efficient* if the time needed to perform the list of instructions can be determined from a polynomial. Devising an efficient algorithm for a given problem is often a difficult task.

The growth rate of running times are typically compared upto constant vectors. Let f and g be defined on some subset of $\mathbb{R}$. $f(x) = O(g(x))$ if and only if there exists a constant M and x_0 such that

$$|g(x)| \leq M\,|f(x)|$$

for all $x \geq x_0$

1.6.1 Complexity Classes

Problems can be categorized by their running times. Each algorithm computes a function $f(I)$ on an input I, however many different algorithms can compute the same function. Algorithms are differentiated by their running times but the function is characterized by the fastest algorithm that can compute it. A problem can be formulated as follows, given input I find $f(I)$.

Problems can be categorized into complexity classes based on the fastest algorithms that solve them. The class of problems that can be solved in polynomial running time is called the *polynomial time* class, P.

A second property of problems is whether its solution can be verified efficiently. This property is independent of whether it can be solved efficiently. B is said to be an *efficient certifier* for a problem X if the following properties hold:

(i) B is a polynomial-time algorithm that takes two inputs s and t.

(ii) There exists a polynomial function p such that for every string s, we have $s \in X$ if and only if there exists a string t such that $|t| \leq p(|s|)$ and $B(s,t) =$ 'yes'.

The class of problems which have an efficient certifier is said to be the *nondeterministic polynomial time* class, NP. We continue with the definitions for NP-hard and NP-complete. A problem is NP-hard if every problem in NP can be reduced to it in polynomial time. A *polynomial time reduction* is when arbitrary instances of problem Y be solved using a polynomial number of standard computational steps, plus a polynomial number of calls to a black box that solves problem X, i.e. Y is reduced in polynomial time to X. A problem is NP-complete if it NP and NP-hard, i.e. NP-complete = NP $\cap$ NP-hard.

1.6.2 RSA Cryptosystem

Cryptography is the study of secure communication between parties in an untrusted or unsecure communication channel. Cryptography has three primary purposes for secure communications: provide confidentiality, authenticate entities, and verification of data. Modern cryptography is based on hard math problems such as integer factorization, discrete logarithmic problem, and pre-image problems. Hard math problems are not found in P and found in NP. In most forms of modern cryptography, *keys*, are data parameters used to form function outputs for the use in a communication channel. There are three common types of keys in cryptography:

1. A *secret key* is known by certain entities. Typically a secret key is used by entities to encrypt and decrypt data that is communicated over an untrusted channel. Secret keys require a secure channel to exchange between all entities.

2. When there are no means to exchange secret keys, one can use a private and public key scheme. A *public key* is a key that can be shared with any entity, i.e. trusted and untrusted entities can know it. The *private key* is a key that is kept to one entity. It is treated like a secret key and should only be known to that entity.

A *cryptosystem* is a suite of algorithms used to establish secure communication channel between parties. The RSA cryptosystem is the first practical cryptosystem in modern cryptography that allows for encryption of

data (confidentiality), authentication of entites, and verify message integrity using just one underlying hard math problem, integer factorization.

RSA is named after its second inventors, Ron Rivest, Adi Shamir, and Leonard Adelmen. These three individuals devised and published the algorithm in 1977. The original inventor of RSA was Clifford Cocks in 1973 however, it was only known to the public since 1997 that Clifford Cocks was the original inventor because his was was classified by Government Communication Headquaters, an intelligence agency of the United Kingdom.

For the RSA cryptosystem, we first want to pose the communication security problem. Suppose we have two entities, Alice and Bob, that wish to communicate over an unsecure channel. Should Alice and Bob agree to using RSA, each entity will have a pair of keys, a private key and a public key. Most implementations of RSA use the following key derivation [19]:

1. Let $n = p \cdot q$ where p and q are randomly chosen prime numbers.
2. Choose an integer e such that $1 < e \leq \phi(n)$ and $gcd\,(e, \phi\,(n)) = 1$ where ϕ is the Euler totient function.
3. Let $d \equiv e^{-1} \mod \phi(n)$.

The RSA cryptosystem is based around the following formula:

$$(m^e)^d \mod n = \left(m^d\right)^e \mod n \equiv m \mod n$$

where we have natural numbers e, d, m, and n, such that $m < n$ and $gcd(m,n) = 1$.

If Alice derives a public and private key in the manner described, her public key is (n,e) and her private key is d. Suppose Bob wants to send Alice a message M. Bob will represent M in binary form, m. Alice sends her public key (n,e) to Bob and keeps her private key d secret. If $gcd(m,n) \neq 1$, then Bob modifies m by padding m with additional digits so that m becomes co-prime with n. There are efficient padding schemes to modify m such that m and n are co-prime [12]. Bob sends the following value, c, to Alice:

$$c \equiv m^e \mod n$$

c is said to be a ciphertext. Alice can decrypt the ciphertext and recover m by computing:

$$m \equiv c^d \mod n = (m^e)^d \mod n$$

The RSA cryptosystem is based on integer factorization and the RSA problem, given n where $n = p \cdot q$ where p and q are prime numbers, find p and q. For sufficiently large integers, factorization and the RSA problem becomes very difficult. If there were an algorithm that solved integer factorization in polynomial time, then one can also solve the RSA problem as well. Suppose a third party listens into the conversation and knows Alice's public key (n,e) and the ciphertext c. If the the third party can factor $n = p \cdot q$ then the attacker can computer $\phi(n)$ and compute $d \equiv e^{-1} \mod \phi(n)$ using the extended euclidian algorithm. Once they have d, the attacker can compute $m \equiv c^d \mod n$.

Currently, the most efficient factorization algorithm is the general number sieve algorithm [16]. It's an exponential running time algorithm. If a polynomial running time algorithm for integer factorization existed, it would allow for compromise of security that is provided to communicating parties by the RSA cryptosystem. It would allow for a reduction of the integer factorization problem, a problem that exists in NP but not P. The algorithm would allow for an adversary to attack RSA [18] in polynomial time.

1.7 Satisfiability

Let $x_1, \ldots, x_n$ be boolean variables. A boolean formula is a combination of conjunction, disjunctions, and negations of the boolean variables $x_1, \ldots, x_n$. A *clause* is a disjunction of distinct literals. A *literal* is a variable or a negated variable, x_i or $\bar{x}_i$, for $i = 1, \ldots, n$. A boolean formula is *satisfiable* if one can assign true or false value to each variable so that the formula is true. It is known that every boolean formula can be rewritten in *conjunctive normal form* (CNF), a conjunction of clauses, via DeMorgan's law and distributive law. Furthermore, it is also known that every boolean formula can be written in CNF such that each clause has exactly three literals. This form is called 3-CNF. For example, consider the clause $A \vee B \vee C \vee D \vee E$. This clause can be rewritten in 3-CNF form as $(A \vee B \vee x_1) \wedge (\neg x_1 \vee C \vee x_2) \wedge (\neg x_2 \vee D \vee E)$ where x_1 and x_2 are literals that allow us to form 3-CNF clauses. Here are the problem statements for satisfiability:

Problem 5 (Satisfiability Problem (SAT)). Given a boolean formula, is it satisfiable? [20]

Brute force is when an algorithm tries all possibilities to see if any formulates a satisfiable solution. It is clear that SAT is decidable in exponential time by testing all possibilities. This is callled a brute force solution. It is not known whether SAT admits a polynomial time solution, that is whether it is in P.

Problem 6 (3-SAT Problem). Given a boolean formula in 3-CNF, is it satisfiable?

The problems we focus on in this thesis have a geometry. A special geometric 3-SAT problem is that Planar 3-SAT Problem. Given a 3-CNF boolean formula, Φ, with n variables and m clauses. We define the *associated graph* $A(\Phi)$ as follows: the vertices correspond to the variables and clauses in Φ. We place an edge in the graph if variable x_i appears in clause C_j.

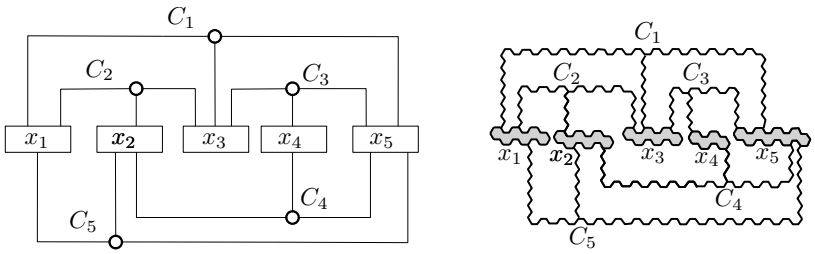

Figure 1.23: Left: the associated graph $A(\Phi)$ for a Boolean formula Φ. Right: the schematic layout of the variable, clause, and transmitter gadgets in the auxiliary construction showing in Section 3.1

Problem 7 (Planar 3-SAT). Given a boolean formula Φ in 3-CNF such that its associated graph is planar, decide whether it is satisfiable is a *3-SAT problem*.

Figure 1.23 is associated to a family of boolean formulas. One such associated boolean formula is:

$$(x_1 \vee x_3 \vee \neg x_5) \wedge (\neg x_1 \vee \neg x_2 \vee x_3) \wedge (\neg x_3 \vee x_4 \vee \neg x_5) \wedge (x_2 \vee x_4 \vee \neg x_5) \wedge (\neg x_1 \vee x_2 \vee x_5)$$

Note that the figure establishes an edge relation between variables and clauses whereas the clauses in boolean formulas do not have variables but literals of variables.

Problem 8 (Not All Equal 3 SAT Problem (NAE3SAT)). Given a boolean formula in 3-CNF, is it satisfiable so that each clause contains a true and a false literal?

Problems 5—8 are known to be NP-hard and are often used to show other problems are NP-hard as well [17, 13].

1.8 Contribution

The *realizability* problem for a polygonal linkage asks whether a given polygonal linkage has a realization (resp., orientated realization). For a weighted planar (resp., plane) graph,, it asks whether the graph is the contact graph (resp., ordered contact graph) of some disk arrangement with specified radii. These problems, in

general, are known to be NP-hard. Specifically, it is NP-hard to decide whether a given planar (or plane) graph can be embedded in $\mathbb{R}^2$ with given edge lengths [7, 10]. Since an edge of given length can be modeled by a suitably long and skinny rhombus, the realizability of polygonal linkages is also NP-hard. The recognition of the contact graphs of unit disks in the plane (a.k.a. coin graphs) is NP-hard [6], and so the realizability of weighted graphs as contact graphs of disks is also NP-hard. However, previous reductions crucially rely on configurations with high genus: the planar graphs in [7, 10] and the coin graphs in [6] have many cycles.

In this thesis, we consider the above four realizability problems when the union of the polygons (resp., disks) in the desired configuration is simply connected (i.e., contractible). That is, the contact graph of the disks is a tree, or the "hinge graph" of the polygonal linkage is a tree (the vertices in the *hinge graph* are the polygons in $\mathscr{P}$, and edges represent a hinge between two polygons). Our main result is that realizability remains NP-hard when restricted to simply connected structures.

Theorem 1. *It is strongly NP-hard to decide whether a polygonal linkage whose hinge graph is a **tree** can be realized.*

Theorem 2. *It is strongly NP-hard to decide whether a polygonal linkage whose hinge graph is a **tree** can be realized with fixed orientation.*

Our proof for Theorem 2 is a reduction from PLANAR-3-SAT (P3SAT): decide whether a given Boolean formula in 3-CNF with a planar associated graph is satisfiable. Our proof for Theorem 8 is a reduction from NOT-ALL-EQUAL-3-SAT (NAE3SAT): decide whether a given Boolean formula in 3-CNF is it satisfiable so that each clause contains a true and a false literal?

Theorem 3. *It is NP-Hard to decide whether a polygonal linkage whose hinge graph is a tree can be realized (both with and without orientation).*

Theorem 4. *It is NP-Hard to decide whether a given tree (resp., plane tree) with positive vertex weights is the contact graph (resp., contact graph) of a disk arrangements with specified radii.*

The unoriented versions, where the underlying graph (hinge graph or contact graph) is a tree can easily be handled with the logic engine method (Section **??**). We prove Theorem 3 for *oriented* realizations with a reduction from PLANAR-3SAT (Section **??**), and then reduce the realizability of ordered contact trees to the oriented realization of polygonal linkages by simulating polygons with arrangements of disks (Section 1.4).

1.9 Related Work and Results

Boris Klemz's Master's thesis "Weighted Disk Contact Graph"..... Breu and Kirkpatrick....

Chapter 2

Decision Problems for Hinged Polygons and Disks

2.1 The Logic Engine

The *logic engine* is a planar, mechanical device that simulates an instance NAE3SAT problem. It was introduced in Bhatt et. al. [4].

2.1.1 Construction of the Logic Engine

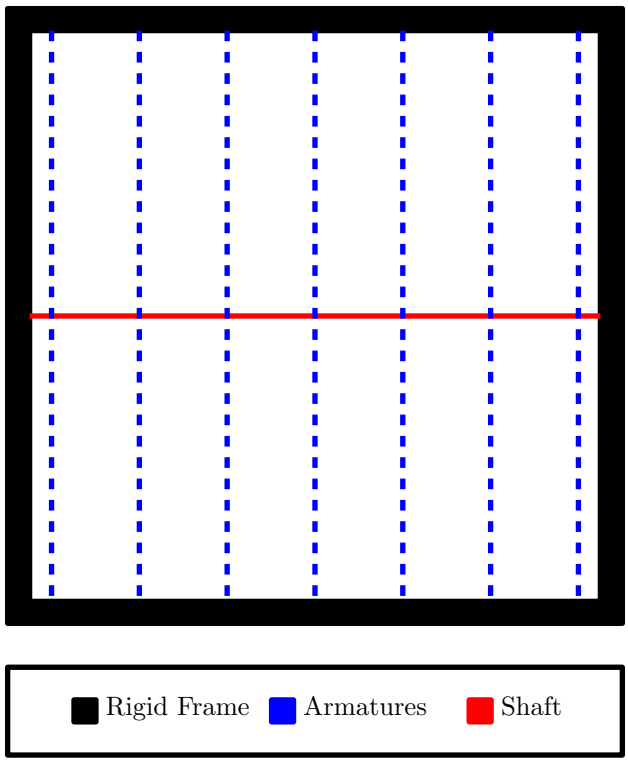

Figure 2.1: A logic engine frame with veritical armatures and a horizontal shaft.

For a given a boolean formula, Φ, in 3-CNF with n variables and m clauses, we construct a logic engine. The logic engine has a *rigid frame* which houses the mechanical components of the the logic engine. The rigid frame is the boundary of which the logic engine can operate within. The *shaft* is a horizontal line segment that is placed at mid-height of the rigid frame. The *armatures* are veritical line segments whose midpoints are on the shaft. Each armature has two orientations with respect to the shaft. There will be some flags on each armature that will be described later. The armatures each have length $2n$ units, the shaft has length m units, and the frame has a height of $2n$ and width of m units.

Each armature corresponds to a variable in Φ. There are two literals for each variable, i.e. the literal x_j and the negated literal $\bar{x}_j$. To describe the flagging arrangement, first partition each armature into $2m$ units, vertical line segments. Label the segments on the j^{th} armature starting from the shaft by $\ell_{j,1},\ldots,\ell_{j,n}$ on one side and $\bar{\ell}_{j,1},\ldots,\bar{\ell}_{j,n}$ on the other side of the shaft. Attach regular triangles, called *flags*, to some of these segments. Each segment is either flagged one or zero flags, i.e. *flagged* or *unflagged*.

1. If the literal x_j is found in clause C_k, then $\ell_{j,k}$ is unflagged.

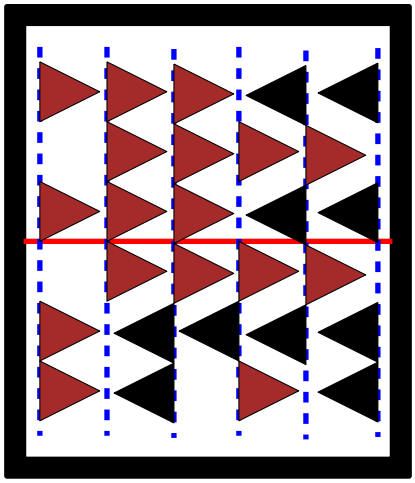

Figure 2.2: A logic engine that corresponds to a boolean formula in NAE3SAT form, Φ. The picture shows the outer rigid frame, the shaft, the armatures that correspond to the variables in Φ, with oriented flags.

2. If the literal $\bar{x}_j$ is found in clause C_k, then $\bar{l}_{j,k}$ is unflagged.

Each flag has two orientations with respect to armature it is attached to. Each flag has four potential positions, the flag can reflect left or right about the armature and the armature can reflect up or down about the shaft. The *flags* are equilateral triangles attached to the armatures. The placement of the flags is dependent

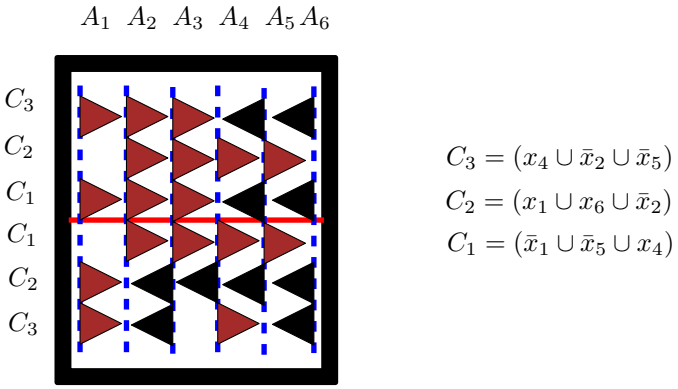

Figure 2.3: A logic engine constructed from the boolean formula $\Phi = C_1 \cap C_2 \cap C_3$.

on the instance of the NAE3SAT boolean formula. Each flag as two orientations.

For the NP hardness reduction in Theorem 6 we need to make sure that all parameters in the logic engine can be specified polynomially in terms of the size of the boolean formula. Given Φ, the corresponding logic engine is constructed as follows: all components will be specified with a quantity and coordinates defined as polynomials in m and n.

2.1.2 The mechanics of the logic engine

In any of the following cases, a *collision* of flags occurs:

Component	Quantity	Set Definition
Rigid Frame	1	$\{ (x,y) \in \mathbb{R}^2 \mid \text{The boundary of } [\frac{1}{2}, n+\frac{1}{2}] \times [-m,m] \}$
Shaft	1	$\{ (x,y) \in \mathbb{R}^2 \mid x \in [\frac{1}{2}, n+\frac{1}{2}] \text{ and } y = 0 \}$
Armatures	n	For the j^{th} armature we have $\{ (x,y) \in \mathbb{R}^2 \mid x = j \text{ and } y \in [-m,m] \}$
Flags	$2mn-3m$	if $\ell_{j,k}$ is flagged then the attached flag is a regular triangle with side length 1.

Table 2.1: The quantity and coordinates of the logic engine components.

1. flags in the same row on adjacent armatures point toward each other.
2. a flag from the rightmost armature A_n points towards the outer rigid frame.
3. a flag from the leftmost armature A_1 points inwards of A_1.

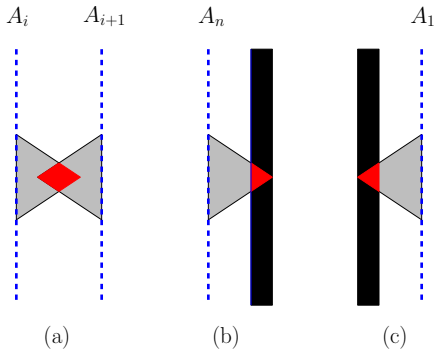

Figure 2.4: (a) Illustrates a adjacent flag collision at the same height, (b) and (c) illustrates a rigid frame collision.

The logic engine representation corresponding to Φ is to be configured such that no horizontally adjacent flags collide and flags do not collide with the rigid frame.

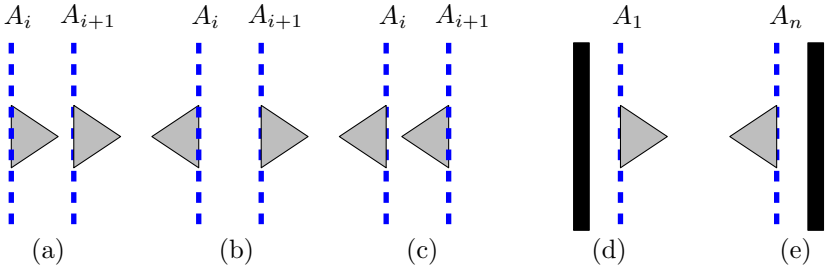

Figure 2.5: The following configuration of adjacent flags and flags that are adjacent to the rigid frame.

Lemma 1. *A row has a collision-free configuration if and only if it has at least one unglagged armature.*

Proof. Suppose all armatures are flagged in a row. The flag on armature A_1 must point to the right otherwise we result in a rigid frame collision. A_2 must point to the right otherwise we result in a rigid frame collision. Without loss of generality, A_i and A_{i+1} must point to the right in order to prevent an adjacent flag collision. This implies that A_n must also point to the right which results into a rigid frame collision.

A same argument holds with the argument beginning with the flag on the armature A_n pointing to the left. Thus there is no collision-free configuration with all armatures flagged.

Suppose there is an unflagged armature in a row. Turn all flags towards the nearest unflagged armature. If there are flags on A_1 and A_n, point toward the interior thus they do not collide with the rigid frame. If there are flags on two consecutive armatures, they do not collide because the nearest unflagged armature cannot be between them. Therefore the row has a collision-free configuration. □

A logic engine is said to be *collision-free configurable* when every row has a collision-free configuration.

2.1.2.1 The Relationship of the Logic Engine and NAE3SAT

We show that given an boolean formula in 3-CNF form, Φ, and a truth assignement, τ, where the variables are given a truth assignment such that there is at least one true literal and one false literal in each clause of Φ, then the corresponding logic engine to Φ is collision-free configurable.

Theorem 5. *Given an instance of a NAE3SAT, it is a "yes" instance if and only if the corresponding logic engine is collision-free configurable.*

Proof. Suppose we have an instance of a *NAE3SAT* that is a "yes" instance. This implies that there is a truth assignment such that each clause contains a true and a false literal. Now consider the logic engine corresponding to this instance. We now show that it has a collision free configuration.

For variables that are true, configure the armatures such that the flags corresponding to the non-negated literals reside above the shaft and the flags that correspond to the negated literals reside below this shaft. For variables that are false, configure the armatures in the opposite orientation. Each clause corresponds to a pair of rows in the logic engine, one row for non-negated literals and one for negated literals. Because the *NAE3SAT* is a yes instance, every row contains at least one unflagged armature. By Lemma 1, every row has a collision-free configuration.

Suppose we have an instance of a *NAE3SAT* such that the corresponding logic engine has a collision-free configuration. By Lemma 1 every row at least one unflagged armature. The k^{th} clause is represented by the k^{th} rows above and below the shaft. If the literal x_j is found in clause C_k, then the armature is unflagged in that row. If the literal $\bar{x}_j$ is found in clause C_k, then $\bar{l}_{j,k}$ is unflagged. All flags corresponding to negated literals reside below the shaft and flags corresponding to non-negated literals reside above the shaft. All together we have that every clause has a true literal and a false literal. Thus, we have a 'yes' instance of the *NAE3SAT*. □

Theorem 6. *Deciding whether a logic engine is collision-free configurable is NP-Hard.*

Proof. In table **??**, we defined the components of the logic engine in terms of polynomials in m and n. If there were a polynomial time algorithm that decides whether a given logic engine is collision-free configurable, then by Theorem 5 we would have a polynomial time algorithm to decide whether an instance of the NAE3SAT is a 'yes' instance. Since NAE3SAT is NP-Hard [11], there is no such algorithm unless $P = NP$. □

2.2 Logic Engines Represented as Polygonal Linkages

In the previous section, we introduced the logic engine. This section builds an analogous structure that is formed from a polygonal linkage and we may interchangeably say subcomponent for polygon. We can modify the mechanical structure of the logic engine to form a polygonal linkage. For a given a boolean formula, Φ, in 3-CNF with n variables and m clauses, the rigid frame is broken into two polygons, each polygon on the extremity of the structure. The shaft is broken into n polygons. Each armature is broken into two parts, each part containing m subcomponents. In figure 2.7, each flag becomes a rectangle.

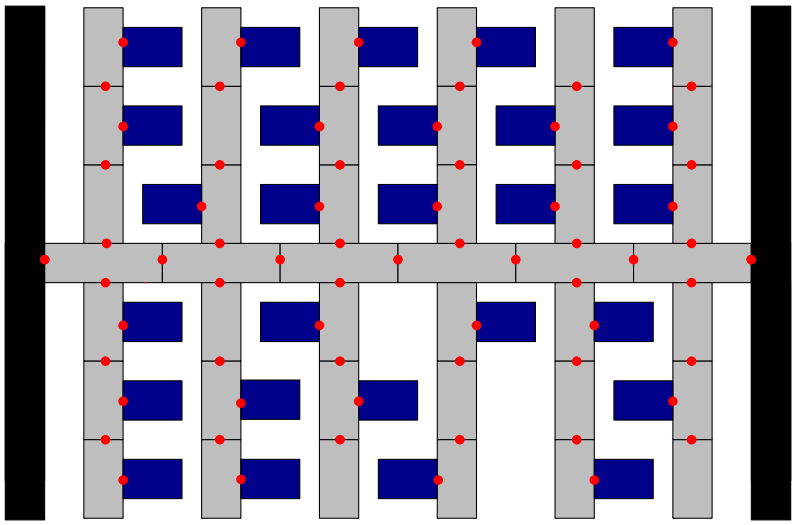

Figure 2.7: A logic engine realized as a polygonal linkage.

2.2.1 Construction of the Polygonal Linkage Logic Engine

Suppose we are given an boolean formula with m clauses and n variables in 3-CNF form, Φ, we construct the polygonal linkage similarly to the logic engine. The corresponding polygonal linkage $P_\ell = (\mathscr{P}, \mathscr{H})$ is detailed in Table **??**.

The large frame subcomponents are hinged on the left most and right most shaft subcomponents. Each adjacent shaft subcomponents are hinged and each shaft subcomponent has two orientations, a reflecion up and a reflection down about the shaft hinge points. On each shaft subcomponent there are two armature shaft subcomponents, one above the shaft subcomponent and one below the shaft subcomponent. By the two orientations of the shaft subcomponent, each armature subcomponent has to possible positions. Each

Component	Height	Width	Quantity
Large Frame Subcomponent	$2 \cdot m$	1	2
Shaft Subcomponent	1	3	n
Armature Subcomponent	2	1	$2 \cdot m$
Flag	1	1.5	$2mn - 3m$

Table 2.2: The components of $\mathscr{P}$ specified polynomially in terms of the size of the boolean formula Φ.

armature comprises of m armature subcomponents that are hinged together; in total there are $2n$ armatures. Each armature subcomponent has two orientations, a reflection left and a reflection right about the armature hinge points. Label the armature subcomponents on the j^{th} armature starting from the shaft by $\ell_{j,1},\ldots,\ell_{j,n}$ on one side and $\bar{\ell}_{j,1},\ldots,\bar{\ell}_{j,n}$ on the other side of the shaft. Attach a rectangular flag specified in Table **??**, to some of these segments. Each segment is either flagged one or zero flags.

1. If the literal x_j is found in clause C_k, then $\ell_{j,k}$ is unflagged.
2. If the literal $\bar{x}_j$ is found in clause C_k, then $\bar{l}_{j,k}$ is unflagged.

Each flag has two orientations with respect to armature it is attached to. Each flag has four potential positions, the flag can reflect left or right about the armature and the armature can reflect up or down about the shaft.

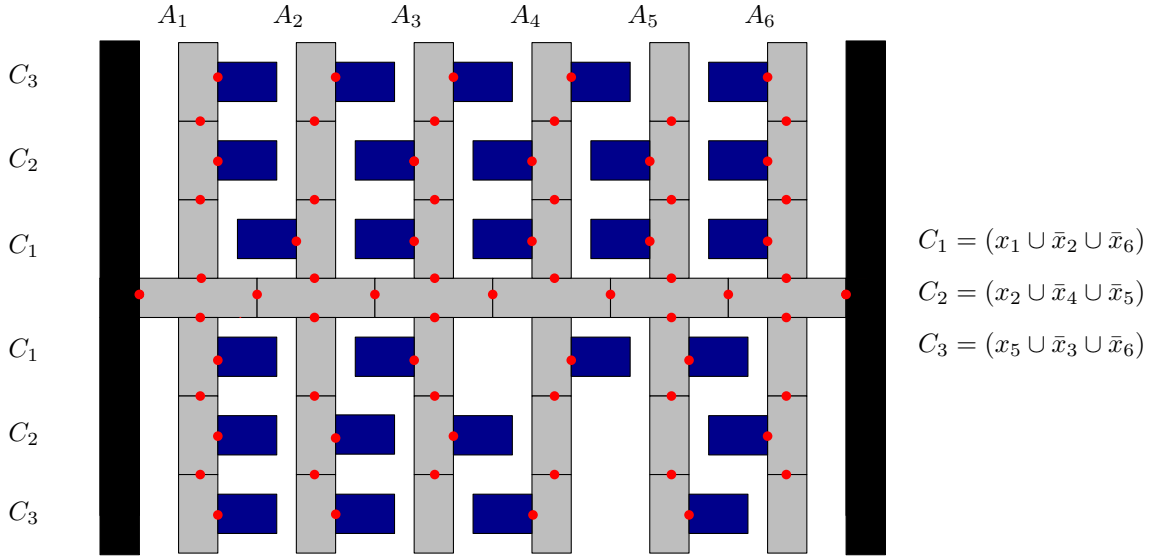

Figure 2.8: A polygonal linkage logic engine that corresponds to the boolean formula $\Phi = C_1 \cap C_2 \cap C_3$.

Theorem 7. *Given an instance of a NAE3SAT, it is a "yes" instance if and only if the corresponding polygonal linkage logic engine has a collision-free configuration.*

Proof. Suppose we have an instance of a *NAE3SAT* that is a "yes" instance. This implies that there is a truth assignment such that each clause contains a true and a false literal. Now consider the polygonal linkage logic engine corresponding to this instance. We now show that it has a collision free configuration.

For variables that are true, configure the armatures such that the flags corresponding to the non-negated literals reside above the shaft and the flags that correspond to the negated literals reside below this shaft. For variables that are false, configure the armatures in the opposite orientation. Each clause corresponds to a pair of rows in the polygonal linkage logic engine, one row for non-negated literals and one for negated literals. Because the *NAE3SAT* is a yes instance, every row contains at least one unflagged armature. By Lemma 1, every row has a collision-free configuration.

Suppose we have an instance of a *NAE3SAT* such that the corresponding polygonal linkage logic engine has a collision-free configuration. By Lemma 1 every row at least one unflagged armature. The k^{th} clause is represented by the k^{th} rows above and below the shaft. If the literal x_j is found in clause C_k, then the armature is unflagged in that row. If the literal $\bar{x}_j$ is found in clause C_k, then $\bar{l}_{j,k}$ is unflagged. All flags corresponding to negated literals reside below the shaft and flags corresponding to non-negated literals reside above the shaft.

All together we have that every clause has a true literal and a false literal. Thus, we have a 'yes' instance of the $NAE3SAT$. □

2.3 Realizability Problems for Weighted Trees

In figure 2.9, we have a set of unit radius disks (circles) arranged in a manner that outlines regular, concentric hexagons.

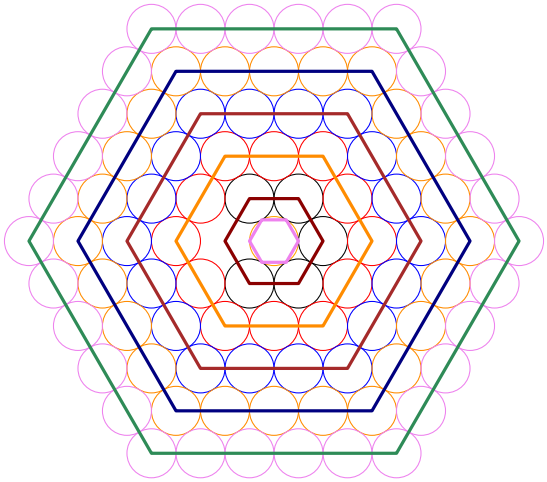

Figure 2.9: A contact graph that resembles the shape of concentric hexagons.

Problem 9 (Appoximating Polygonal Shapes with Contact Graphs). For every $\varepsilon > 0$ and polygon P, there exists a contact graph $G = (V,E)$ such that the Hausdorff distance $d(P,G) < \varepsilon$

Recall problems (**??**) and (**??**): given a positive weighted tree, T, is T the (ordered) contact graph of some disk arrangement where the radii are equal to the vertex weights. For now, we'll focus on a particular family of this problem space where the weighted trees can be realized as a *snowflake*. For $i \in \mathbb{N}$, the construction of the snowflake tree, S_i, is as follows:

- Let v_0 be a vertex that has six paths attached to it: p_1, p_2, ..., p_6. Each path has i vertices.
- For every other path p_1, p_3, and p_5:
  - Each vertex on that path has two paths attached, one path on each side of p_k.
  - The number of vertices that lie on the path attached to the j^{th} vertex of p_k is $i - j$.

A *perfectly weighted snowflake tree* is a snowflake tree with all vertices having weight $\frac{1}{2}$. A *perturbed snowflake tree* is a snowflake tree with all vertices having weight of 1 with the exception of v_0; in a perturbed snowflake tree, v_0 will have a radius of $\frac{1}{2} + \gamma$. For our analysis, all realizations of any snowflake, perfect or perturbed, shall have v_0 fixed at origin. This is said to be the canonical position under Hausdorff distance of the snowflake tree.

Consider the graph of the triangular lattice with unit distant edges:

$$\begin{aligned} V &= \left\{ a \cdot (1,0) + b \cdot \left(\frac{1}{2}, \frac{\sqrt{3}}{2} \right) : a,b \in \mathbb{Z} \right\} \\ E &= \{\{u,v\} : ||u-v|| = 1 \text{ and } u,v \in V\} \end{aligned}$$

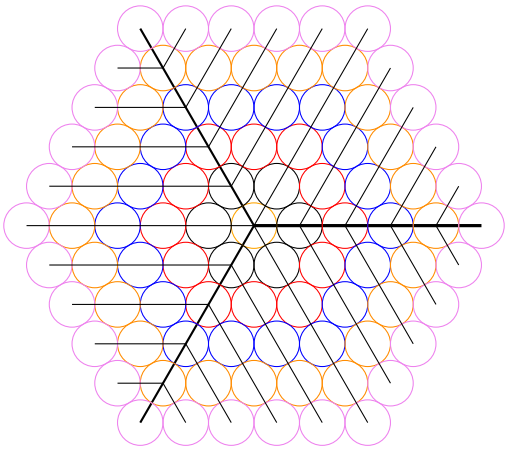

Figure 2.10: The same contact graph as in figure 2.9 overlayed with the a perfectly weighted snowflake tree.

The following graph, $G = (V,E)$ is said to be the *unit distance graph* of the triangular lattice. We can show that no two distinct edges of this graph are non-crossing. First suppose that there were two distinct edges that crossed, $\{u_1, v_1\}$ and $\{u_2, v_2\}$. With respect to u_1, there are 6 possible edges corresponding to it, with each edge $\frac{\pi}{3}$ radians away from the next. Neither edge crosses another; and so we have a contradiction that there are no edge crossings with $\{u_1, v_1\}$.

The perfectly weighted snowflake tree that is a subgraph over the *unit distance graph*, $G = (V,E)$, of the triangular lattice. To show this, for any S_i, fix $v_0 = 0 \cdot \cdot (1,0) + 0 \cdot \left(\frac{1}{2}, \frac{\sqrt{3}}{2}\right) = (0,0) \in V$ at origin. Next consider the six paths attached from origin. Fix each consecutive path $\frac{\pi}{3}$ radians away from the next such that the following points like on the corresponding paths: $(1,0) \in p_1, \left(\frac{1}{2}, \frac{\sqrt{2}}{3}\right) \in p_2, \left(-\frac{1}{2}\mathsf{p}_4, \frac{\sqrt{3}}{2}\right) \in p_3, (-1,0) \in p4, \left(-\frac{1}{2}, -\frac{\sqrt{3}}{2}\right) \in p_5, \left(\frac{1}{2}, -\frac{\sqrt{3}}{2}\right) \in p_6$. For S_i, there are i vertices on each path.

We define the six paths from origin as follows:

$$
\begin{aligned}
p_1 &= \left\{ a \cdot (1,0) = \vec{v} \middle| a \in \mathbb{R}^+ \right\} \\
p_2 &= \left\{ a \cdot \left(\frac{1}{2}, \frac{\sqrt{3}}{2}\right) = \vec{v} \middle| a \in \mathbb{R}^+ \right\} \\
p_3 &= \left\{ -a \cdot (1,0) + a \cdot \left(\frac{1}{2}, \frac{\sqrt{3}}{2}\right) = a \left(-\frac{1}{2}, \frac{\sqrt{3}}{2}\right) = \vec{v} \middle| a \in \mathbb{R}^+ \right\} \\
p_4 &= \left\{ a \cdot (-1,0) = \vec{v} \middle| a \in \mathbb{R}^+ \right\} \\
p_5 &= \left\{ a \cdot \left(-\frac{1}{2}, -\frac{\sqrt{3}}{2}\right) = \vec{v} \middle| a \in \mathbb{R}^+ \right\} \\
p_6 &= \left\{ a \cdot (1,0) - a \cdot \left(\frac{1}{2}, \frac{\sqrt{3}}{2}\right) = a \cdot \left(\frac{1}{2}, -\frac{\sqrt{3}}{2}\right) \middle| a \in \mathbb{R}^+ \right\}
\end{aligned}
$$

For S_i there exists i vertices on each path. We shall denote the i^{th} vertex on the j^{th} path as $v_{j,i}$. For each path defined above, the paths are defined as a set of vectors, $\vec{v} = a \cdot \vec{p}$ for some $a \in \mathbb{R}^+$ and $\vec{p} \in \mathbb{R}^2$. By setting $a = 1, 2, \ldots, i$, we obtain points that are contained in V. For $j = 1, 3, 5$ and $l = 1, ..., i$, there exists two paths attached to each vertex $v_{j,l}$. For S_i, each path attached to the k^{th} vertex of p_j, there are $i - k$ vertices. We will need to show that each of the $i - k$ vertices on each corresponding path are also in V.

The triangular lattice is symmetice under rotation about v_0 by $\frac{\pi}{3}$ radians. For each vertex $v_{1,l}$ for $l = 1,2,...,i-k$, we place two paths from it; the first path $\frac{\pi}{3}$ above p_1 at $v_{1,l}$ and $\frac{-\pi}{3}$ below p_1 at $v_{1,l}$ and call these paths $p^+_{1,l}$ and $p^-_{1,l}$ respectively. With respect to $v_{1,l}$, one unit along $p^+_{1,l}$ is a point on the triangular lattice and similarly so on $p^-_{1,l}$. Continuing the walk along these paths, unit distance-by-unit distance, we obtain the next point corresponding point on the the triangular lattice up to $i-k$ distance away from $v_{1,l}$. This shows that each of the $i-k$ vertices on $p^-_{1,l}$ and $p^+_{1,l}$ are in V. By rotating all of the paths along p_1 by $\frac{2\pi}{3}$ and $\frac{4\pi}{3}$, we obtain the the paths along p_3 and p_5 respectively, completing the construction.

2.3.1 On the Decidability of Problem 3

Proof. Consider a $k \times (\sqrt{3}k)$ rectangle section of a triangular lattice, and place disks of radius 1 at each grid point as in Fig. ?????. The contact graph of these disks contains 2-cycles. Consider the spanning tree T of the contact graph indicated in Fig. ????. The tree T decomposes into paths of collinear edges: T contains two paths along the two main diagonals, each containing $2k-1$ vertices; all other paths have an endpoint on a main diagonal. We now modify the disk arrangement to ensure that its contact graph is T. The disks along the main diagonal do not change. We reduce the radii of all other disks by a factor of $1-k^{-3}$ (as a result, they lose contact with other disks), and then successively translate them parallel in the direction of the shortest path in T to the main diagonal until the contact with the adjacent disk is reestablished. The Hausdorff distance between the union of these disks and the initial $k \times (\sqrt{3}k)$ rectangle is clearly less than 1. However, the contact tree T with these radii no longer has a unique realization (small perturbations are possible). To show stability, we argue by induction on the hop distance from the central disk. There are $O(i)$ disks at i hops from the central disk, most one which have radius $(1-k^{-3})\frac{1}{2}$. Since all radii are 1 or $(1-k^{-3})\frac{1}{2}$,the six neighbors of the central disk can differ from the regular hexagon by at most $O(k)$. Similarly, the disks at i hops from the center be off from the triangular grid pattern by $O(i2^{k-3})$, for $i = 1,2,\ldots,k$. □

Chapter 3

Realizability of Polygonal Linkages with Fixed Orientation

We begin the chapter with describing several gadgets that translates the associated graph $A(\Phi)$ of a planar 3SAT instance. These gadgets will be used together to form a special hexagonal tiling that behaves in a similar nature to the logic engine of Chapter 2 but simulate a Planar 3-SAT and its associated graph. Together the gadgets will form what is called the auxilary construction. The hexagonal tiling would then be used to prove the following theorem:

Theorem 8. *It is strongly NP-hard to decide whether a polygonal linkage whose hinge graph is a **tree** can be realized with counter-clockwise orientation.*

Modifying the Associated Graph of a P3SAT Given a P3SAT of n variables and m clauses with associated graph $A(\Phi)$. We construct a finite *honeycomb* grid $H_{A(\Phi)}$ of regular hexagons over the plane centered at origin. Each hexagon of $H_{A(\Phi)}$ is of unit side length and has a polynomial number of hexagons, $s(n,m)$. It is known that the size of the honeycomb is finite and can be determined by polynomials $h(n,m) \times w(n,m)$ [5]. Let $D = \max degree(V)$ where V is the set of vertices of $A(\Phi)$. We modify the associated graph drawing $A(\Phi)$ by overlaying it onto a honeycomb in the following way:

1. **Variable:** A vertex representing a variable shall encompass a horizontally consecutive set of hexagons in the honeycomb. Every variable vertex v must encompass at least $degree(v)$ consecutive hexagons but can encompass upto Dnumber of consecutive hexagons where V is the set of vertices in $A(\Phi)$.
2. **Clause:** A vertex representing a clause shall be a vertex of a hexagon in the honeycomb.
3. **Edge:** Edges of the associated graph $A(\Phi)$ are paths from the variable x_i and clause C_j. An edge $\{x_i, C_j\}$ of the associated graph is pariwise edge disjoint. An edge of the drawing shall traverse the edges of hexagons in a vertically or horizontally zigzagging manner in the honeycomb from the literal to the corresponding clause. The edges are drawn in a manner that best represents an orthogonal graph drawing over the honeycomb. The length of the edges are bounded above by $6 \cdot (\ell_1(x_i, C_j) + D)$. Edges traverse a hexagon in two edges vertically, three edges horizontally. When the edge transisitions from a vertical to horizontal traversal, the edge traverses in over 4 edges about the hexagon.

Figure 3.1 illustrates an associated graph of a P3SAT overlayed on a honeycomb.

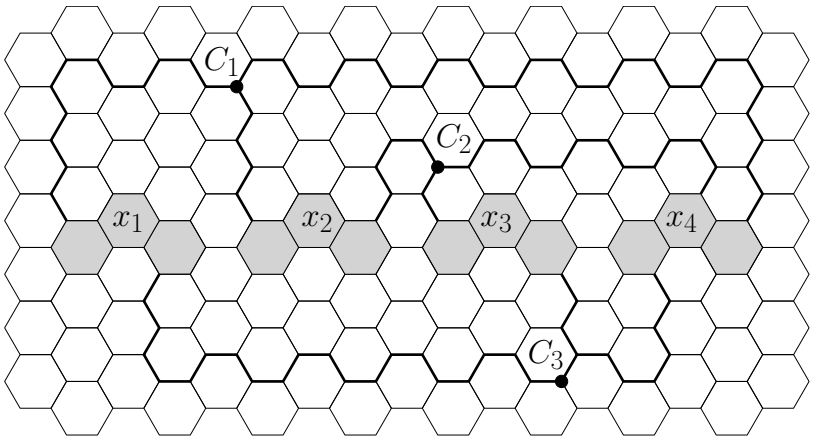

Figure 3.1: This is an instance of an associated graph for a P3SAT overlayed onto a honeycomb grid. This honeycomb graph could correspond to Boolean formula $(\neg x_1 \vee \neg x_2 \vee x_4) \wedge (x_2 \vee \neg x_3 \vee x_4) \wedge (x_1 \vee \neg x_3 \vee \neg x_4)$.

The honeycomb construction will act as preliminary concept that will be refined further in the Auxilary Contruction. We denote the associated graph overlayed on the honeycomb as $\tilde{A}(\Phi)$.

3.1 Auxilary Construction

Given an instance Φ of P3SAT with n variables and m clauses and its associated graph $A(\Phi)$, we construct a simply connected polygonal linkage $(\mathscr{P}, H)$, of polynomial size in n and m, such that Φ is satisfiable if and only if $(\mathscr{P}, H)$ admits a realization with fixed orientation.

We construct a polygonal linkage in two main steps: first, we construct an auxiliary structure where some of the polygons have fixed position in the plane (called *obstacles*), while other polygons are flexible, and each flexible polygon is hinged to an obstacle. Second, we modify the auxiliary construction into a polygonal linkage by allowing the obstacles to move freely, and by adding new polygons and hinges as well as an exterior *frame* that holds the obstacle polygons in place. All polygons in our constructions are regular hexagons or long and skinny rhombi because these are the polygons that we can "simulate" with disk arrangements in Section 1.4.

Let Φ be a Boolean formula of P3SAT with variables $x_1, \ldots, x_n$ and clauses $C_1, \ldots, C_m$, where $A(\Phi)$ is the associated planar graph and $\tilde{A}(\Phi)$ be corresponding honeycomb graph. We continue to modify $\tilde{A}(\Phi)$ to form the auxilary construction. For each hexagon in $\tilde{A}(\Phi)$, we scale the hexagons in the following way: first we fix the center of the hexagon and then scale (shrink) the hexagon; the hexagons in the honeycomb no longer touch each other and form corridors and junctions between the hexagons. Formally, let a *corridor* be a channel between two adjacent hexagons and a *junction* be a region where three corridors meet. We then finally re-scale this form of the honeycomb such that the side length of the hexagons are determined by polynomial of variable n and m, $N(n,m)$, while preserving the corridors formed from the first scaling.

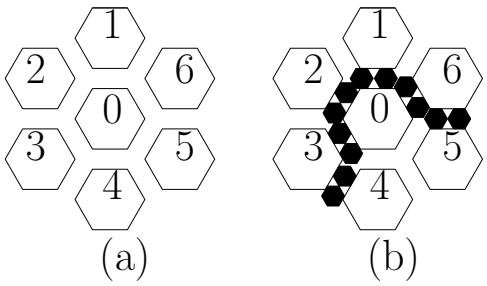

Figure 3.2: (a) A region of the honeycomb shown with scaling. The corridors and junctions formed from the first scaling is preserved after scaling the honeycomb grid to where the side lengths of the hexagon are $N(n,m)$. (b) The same region in (a) containing flexible hexagons.

Let the hexagons of Figure 3.2(a) be obstacle hexagons that are fixed at their centers. In Figure 3.2(b), we have smaller hexagons within some corridors and junctions. These hexagons are flexible hexagons. For each edge in $\tilde{A}(\Phi)$, we will replace that edge with flexible hexagons. Flexible hexagons are hinged at the vertex closest to origin and the side of the corridor (See Figure 3.3). Let $t = 2N^3 + 1$ be the number of flexible hexagons in a corridor (see Figure 3.3). Scale the honeycomb such that the obstacle hexagons become regular hexagons of side length $(5t-1)/2 + \sqrt{3}$, and then scale each obstacle hexagon independently from its center to a hexagon of side length $(5t-1)/2$ (see Figure 3.4).

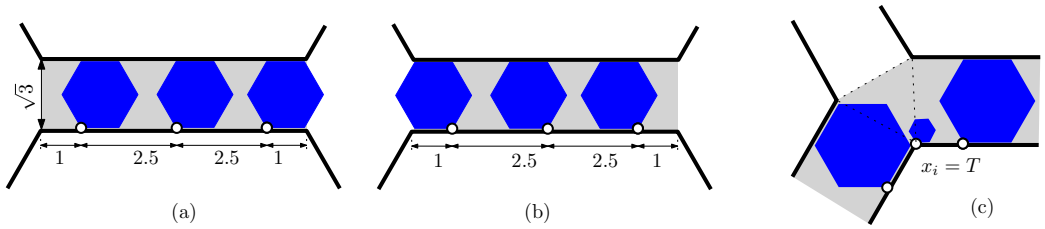

Figure 3.3: (a) A corridor when all unit hexagons are in state R. (b) A corridor where all unit hexagons are in state L. (c) A junction where a small hexagon between two corridors ensures that at most one unit hexagon enters the junction from those corridors.

Between two adjacent obstacle hexagons, there is a $\frac{5t-1}{2} \times \sqrt{3}$ rectanglar corridor. Three adjacent corridors meet at a regular triangle, which we call a *junction*. We next describe variable, clause, and transmitter gadgets.

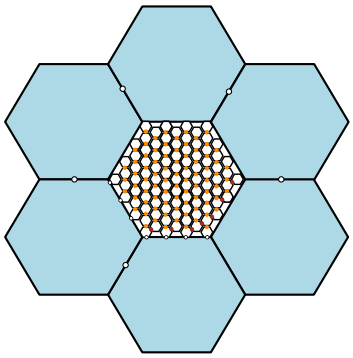

Figure 3.4: The small honeycomb-like structure within the large hexagons depicts cells.

The basic building block of both variable and transmitter gadgets consists of t regular hexagons of side length 1 (*unit hexagons*, for short) attached to a wall of a corridor such that the hinges divide the wall into $t+1$ intervals of length $(1, 2.5, \ldots, 2.5, 1)$ as shown in Fig. 3.3(a-b) for $t = 3$. Since the height of the corridor is $\sqrt{3}$, each hexagon has exactly two possible realizations: it can lie either *left* or *right* of the hinge in a horizontal corridor. For simplicity, we use the same notation (R and L) in nonhorizontal corridors, too. Hence, the *state* of each flexible hexagon in a realization is either L or R. The following observation describes the key mechanism of a corridor.

Observation 1. (1) If the leftmost hexagon is in state R, then all t hexagons are in state R, and the rightmost hexagon enters the junction on the right of the corridor.

(2) Similarly, if the rightmost hexagon is in state L, then all t hexagons are in state L, and the leftmost hexagon enters the junction on the left of the corridor.

Each junction is a regular triangle, adjacent to three corridors. In some of the junctions, we attach a small hexagon of side length $\frac{1}{3}$ to one or two corners of the junction (see Fig. 3.3(c) and Fig. 3.6). Importantly, if such a small hexagon is attached to a vertex between two corridors, then a unit hexagon can enter the junction from at most one of those corridors.

3.1.1 Variable Gadget

The **variable gadget** for variable x_i is constructed as follows. Recall that variable x_i corresponds to a cycle in the associated graph $\tilde{A}(\Phi)$, which has been embedded as a cycle in the hexagonal tiling, with corridors and junctions. In each junction along this cycle, attach a small hexagon in the common boundary of the two corridors in the cycle. Figure 3.5 depicts a *variable gadget* in the hexagonal grid.

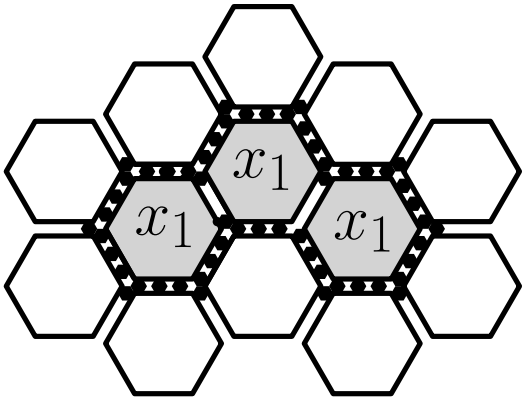

Figure 3.5: This depicts a variable gadget with $x_1 = T$. Carefully note that the flexible hexagons around x_1 are in the state R. Corridors adjacent to two obstacles of a variable in the honeycomb do not have t flexible hexagons; these corridors simply have the flexible hexagons at the junctions.

Observation 1 and the small hexagons ensure that the state of any unit hexagon along the cycle determines the state of all other unit hexagons in the cycle. This property defines the binary variable x_i: If $x_i = T$, then all unit hexagons in the top horizontal corridors are in state R; and if $x_i = F$, they are all in state L.

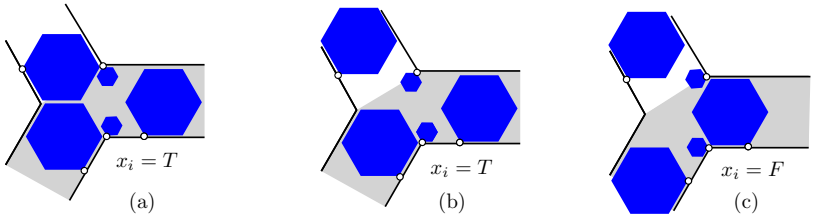

Figure 3.6: The common junction of a variable gadget and a transmitter gadget. (a) When $x_i = T$, a hexagon of the transmitter may enter the junction of the variable gadget. (b) When $x_i = T$, the transmitter gadget has several possible realizations. (c) When $x_i = F$, no hexagon from the transmitter enters a junction of the variable gadget.

3.1.2 Transmitter Gadget

A **transmitter gadget** is constructed for each edge (x_i, C_j) of the graph $A(\Phi)$. It connects a junction of the variable gadget x_i with the junction representing the clause gadget C_j. The gadget consists of a path of corridors and junctions: at each interior junction, attach a small hexagon in the common boundary of the two corridors in the path (similarly to the variable gadget). At the common junction with the variable gadget x_i, we attach one additional small hexagon to one of the vertices (refer to Fig. 3.6). If the literal x_i (resp., $\overline{x}_i$) appears in C_j, then we attach a small hexagon to the corner of this junction such that if $x_i = F$ (resp., $\overline{x}_i = F$), then the unit hexagon of the transmitter gadget cannot enter this junction. This ensures that false literals are always correctly transmitted to the clause junctions (and true literals can always transmit correctly).

3.1.3 Clause Gadget

The **clause gadget** lies at a junction adjacent to three transmitter gadgets (see Fig. 3.7). At such a junction, we attach a unit line segment to an arbitrary vertex of the junction, and a small hexagon of side length $\frac{1}{3}$ to the other end of the segment. If unit hexagons enter the junction from all three corridors (i.e., all three literals are false), then there is no space left for the small hexagon. But if at most two unit hexagons enter the junction (i.e., one of the literals is true), then the unit segment and the small hexagon are realizable.

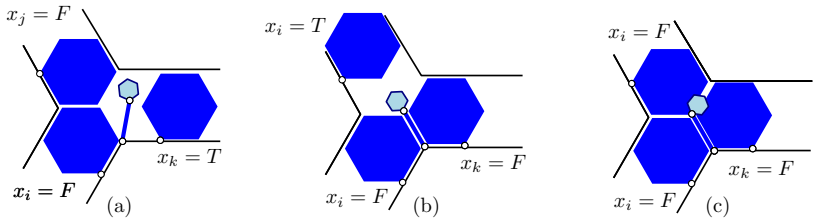

Figure 3.7: (a-b) A clause gadget $(x_i \vee x_j \vee x_k)$ is realizable when at least one of the literals is TRUE. (c) The clause gadget cannot be realized when all three literals are FALSE.

The following lemma summarizes our result about the auxiliary construction.

Lemma 2. *For every instance Φ of P3SAT, the above polygonal linkage with flexible and obstacle polygons has the following properties: (1) it has polynomial size; (2) its hinge graph is a forest; (3) it admits a realization such that the obstacle polygons remain fixed if and only if Φ is satisfiable.*

Proof. Let Φ be an instance of P3SAT (i.e., a Boolean formula Φ in 3-CNF with n variables, m clauses, and a planar graph $A(\Phi)$). We construct a simply connected polygonal linkage $(\mathscr{P}, H)$ that has a realization with fixed orientation iff Φ is satisfiable.

We modify the auxiliary construction allowing all polygons to move freely, and by adding extra polygons and hinges so that the hinge graph becomes a *tree*, and the size of the construction remains polynomial. Recall that our auxiliary construction is based on a polynomial section of the hexagonal tiling, using obstacle hexagons of side lengths $(5t-1)/2$, unit hexagons (of side length 1), and small hexagons of side length $\frac{1}{3}$. We modify it in 3 steps as follows.

1. Move the obstacle hexagons apart such that the width of each corridor increases from $\sqrt{3}$ to $\sqrt{3}+1/(100N)$.
2. Replace the unit segment in each the clause gadget by a skinny rhombus of diameter 1.1 and width $1/(200N)$.
3. Consider a large (polynomial-size) regular hexagon R that contains all gadgets in our construction, and enclose R by a *frame* of 6 congruent regular hexagons, as shown in Fig. 3.8(a), hinged together in a path.
4. Connect the frame and the obstacles in R into a simply connected polygonal linkage: In each obstacle hexagon, the bottom or bottom-left side is adjacent to the frame or to a corridor. Introduce a hinge at the midpoint of one such side in each obstacle hexagon. If this side is adjacent to the frame, then attach the hinge to the frame. Otherwise, the hinge is attached to a new *connector* polygon: a skinny rhombus of diameter 1 and width $1/(200N)$. The far corner of each rhombus is hinged to the unit hexagon in the middle of the corridor at shown in Fig. 3.8(b).

We obtain a simply connected polygonal linkage. We now allow the "obstacle" hexagons to move freely, and call their original fixed position *canonical*. We may assume w.l.o.g. that the frame is at its original position. It is enough to show that the obstacle hexagons are still confined to an $1/N$-neighborhood of their canonical position, then it follows that the polygonal linkage is realizable if and only if Φ is satisfiable. □

The modification of the auxiliary construction is a tree. Satisfiability is an NP-hard problem [9]. Thus, we prove Theorem 8

The obstacle hexagons in the bottom and bottom-left rows are hinged directly to the frame, and so they are locked in their canonical position. Consider two obstacle hexagons on opposite sides of a corridor with connector. The distance between the midpoints of the opposite sides of the corridor is at least $\sqrt{3}$ (due to

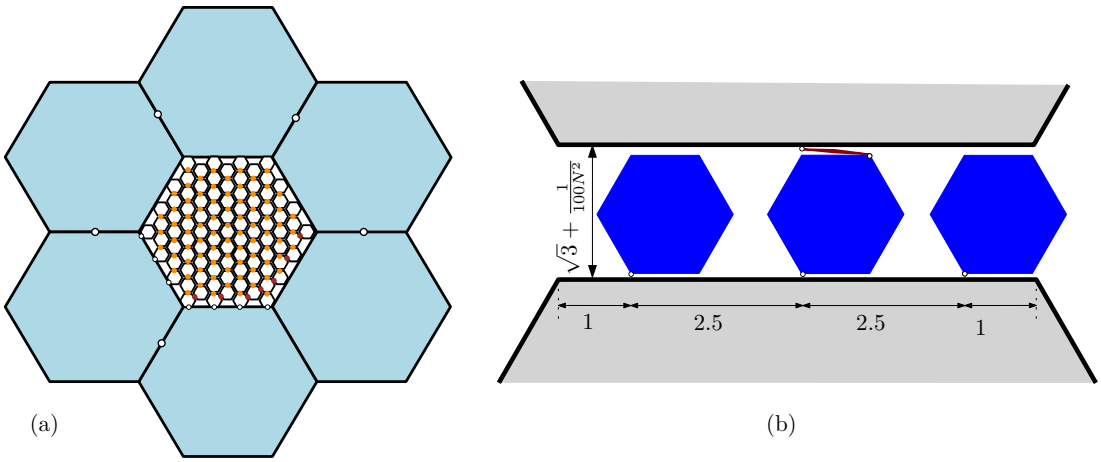

Figure 3.8: (a) A frame (built of 6 hinged regular hexagons) encloses a hexagonal tiling, and vertical paths connect all obstacle hexagons to the frame. (b) A corridor is widened to $\sqrt{3}+1/N^2$. A connection between two adjacent obstacle hexagons is established via a skinny rhombus.

the unit hexagons in the corridor) and at most $1+\sqrt{3}$ (due to the connector polygon). The length of the corridor is much larger, $(5t-1)/2 = 5N^3+2$, so the orientations of the two adjacent obstacles differ by at most $1/2N^3$. Consequently, the orientation of *any* obstacle differs from canonical by at most $1/2N^2$. Due to the unit hexagons within the horizontal corridors, the length of any vertical segment between the opposite sides of a horizontal corridor is at least $1-1/N^2$. The vertical distance between the bottom and top sides of the frame gives an upper bound of $2N/(100N^2) = 1/(50N)$ for the sum of these vertical distances. We conclude that the y-coordinates of the obstacles are within $1/(10N)$ of the canonical position. Due to the connector polygons, the x-coordinates of two adjacent obstacles differ by either less than the vertical offset or by about one unit. However, the horizontal distance between the left and right frames prevent a shift of this magnitude. So the x-coordinates of the obstacle hexagons are also within $1/N$ of the canonical position.

Chapter 4

Disk Arrangement

4.1 Properties for Weighted Trees and Polygonal Linkages

In order to perform our analysis for weighted trees and polygonal linkages, we'll want to use a suitable metric. The usual Euclidian distance will not suffice for this analysis and so we turn to the Hausdorff distance.

Hausdorff Distance Let A and B be sets in the plane. The *directed Hausdorff distance* is

$$d(A,B) = \sup_{a \in A} \inf_{b \in B} ||a-b|| \tag{4.1}$$

$h(A,B)$ finds the furthest point *ainA* from any point in B. *Hausdorff distance* is

$$D(A,B) = \max\{d(A,B), d(B,A)\} \tag{4.2}$$

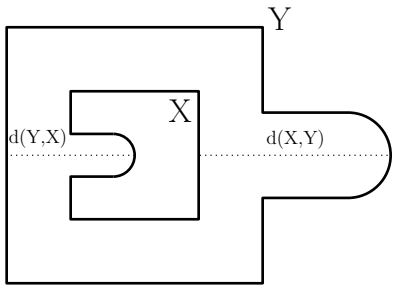

Figure 4.1: An illustrative example of $d(X,Y)$ and $d(Y,X)$ where X is the inner curve, and Y is the outer curve.

ε-approximation The weighted graph, G, is an *ε-approximation* of a polygon P if the Hausdorff distance between every realization such realization of G as a contact graph of disks and a congruent copy of P is at most epsilon. A weighted graph G is said to be a *$O(f(x))$-approximation* of a polygon P if there is a positive constant M such that for all sufficiently large values of x the Hausdorff distance between every realization such realization of G as a contact graph of disks and a congruent copy of P is at $M \cdot |f(x)|$. A weighted graph G is said to be a *stable* if it has the property that for every two such realizations of G, the distance between the centers of the corresponding disks is at most ε after a suitable rigid transformation.

Bibliography

[1] Timothy G Abbott, Zachary Abel, David Charlton, Erik D Demaine, Martin L Demaine, and Scott Duke Kominers. Hinged dissections exist. *Discrete & Computational Geometry*, 47(1):150–186, 2012.

[2] Martin Aigner and Günter M Ziegler. Hilbert's third problem: decomposing polyhedra. *Proofs from the book*, pages 53–61, 2010.

[3] G. Di Battista, P. Eades, R. Tamassia, and I. G. Tollis. *Graph Drawing: Algorithms for the Visualization of Graphs*. Prentice Hall, 1999.

[4] Sandeep N Bhatt and Stavros S Cosmadakis. The complexity of minimizing wire lengths in vlsi layouts. *Information Processing Letters*, 25(4):263–267, 1987.

[5] Therese Biedl and Goos Kant. A better heuristic for orthogonal graph drawings. *Computational Geometry*, 9(3):159–180, 1998.

[6] H. Breu and D. G. Kirkpatrick. Unit disk graph recognition is NP-hard. *Comput. Geom*, 9:3–24, 1998.

[7] R. Connelly, E. D. Demaine, M. L. Demaine, S. P. Fekete, S. Langerman, J. S. B. Mitchell, A. Ribó, and G. Rote. Locked and unlocked chains of planar shapes. *Discrete Comput. Geom*, 44:439–462, 2010.

[8] R. Connelly, E. D. Demaine, and G. Rote. Straightening polygonal arcs and convexifying polygonal cycles. *Discrete Comput. Geom*, 30:205–239, 2003.

[9] Stephen A Cook. The complexity of theorem-proving procedures. In *Proceedings of the third annual ACM symposium on Theory of computing*, pages 151–158. ACM, 1971.

[10] P. Eades and N. C. Wormald. Fixed edge-length graph drawing is NP-hard. *Discrete Applied Mathematics*, 28:111–134, 1990.

[11] Michael R Garey and David S Johnson. *Computers and Intractibility*. WH Freeman and company New York, 1979.

[12] J Jonsson and B Kaliski. Public-key cryptography standards (pkcs)# 1: Rsa cryptography specifications, version 2.1. internet request for comments 3447 (rfc 3447), 2003.

[13] Richard M Karp. *Reducibility among combinatorial problems*. Springer, 1972.

[14] Paul Koebe. *Kontaktprobleme der konformen Abbildung*. Hirzel, 1936.

[15] Casimir Kuratowski. Sur le probleme des courbes gauches en topologie. *Fundamenta mathematicae*, 1(15):271–283, 1930.

[16] Arjen K Lenstra, Hendrik W Lenstra Jr, Mark S Manasse, and John M Pollard. *The number field sieve*. Springer, 1993.

[17] David Lichtenstein. Planar formulae and their uses. *SIAM journal on computing*, 11(2):329–343, 1982.

[18] Alfred J Menezes, Paul C Van Oorschot, and Scott A Vanstone. *Handbook of applied cryptography*. CRC press, 1996.

[19] Ronald L Rivest, Adi Shamir, and Len Adleman. A method for obtaining digital signatures and public-key cryptosystems. *Communications of the ACM*, 21(2):120–126, 1978.

[20] S.S. Skiena. *The Algorithm Design Manual*. Springer, 2009.

[21] I. Streinu. Pseudo-triangulations, rigidity and motion planning. *Discrete Comput. Geom*, 34:587–635, 2005.

[22] E. C. Zeeman. On hilbert's third problem. *The Mathematical Gazette*, 86(506):241–247, 2002.